

# Higgs boson enhancement effects on squark-pair production at the LHC

Abdesslam Arhrib<sup>1,2</sup>, Rachid Benbrik<sup>3,4</sup>, Kingman Cheung<sup>5,6,7</sup> and Tzu-Chiang Yuan<sup>8</sup>

<sup>1</sup> *Département de Mathématiques, Faculté des*

*Sciences et Techniques, B.P 416 Tangier, Morocco*

<sup>2</sup> *Department of Physics, National Taiwan University, Taipei, Taiwan*

<sup>3</sup> *Department of Physics, National Cheng Kung University, Tainan 701, Taiwan*

<sup>4</sup> *National Center for Theoretical Physics, Tainan 701, Taiwan*

<sup>5</sup> *Division of Quantum Phases & Devices, School of Physics,*

*Konkuk University, Seoul 143-701, Korea*

<sup>6</sup> *Department of Physics, National Tsing Hua University, Hsinchu, Taiwan*

<sup>7</sup> *Physics Division, National Center for Theoretical Sciences, Hsinchu, Taiwan*

<sup>8</sup> *Institute of Physics, Academia Sinica, Nankang, Taipei 11529, Taiwan*

(Dated: November 2, 2018)

## Abstract

We study the Higgs boson effects on third-generation squark-pair production in proton-proton collision at the CERN Large Hadron Collider (LHC), including  $\tilde{t}\tilde{t}^*$ ,  $\tilde{t}\tilde{b}^*$ , and  $\tilde{b}\tilde{b}^*$ . We found that substantial enhancement can be obtained through  $s$ -channel exchanges of Higgs bosons at large  $\tan\beta$ , at which the enhancement mainly comes from  $b\bar{b}$ ,  $b\bar{c}$ , and  $c\bar{b}$  initial states. We compute the complete set of electroweak (EW) contributions to all production channels. This completes previous computations in the literature. We found that the EW contributions can be significant and can reach up to 25% in more general scenarios and at the resonance of the heavy Higgs boson. The size of Higgs enhancement is comparable or even higher than the PDF uncertainties and so must be included in any reliable analysis. A full analytical computation of all the EW contributions is presented.

PACS numbers: 12.60.Jv, 14.80.Da, 14.80.Ly

## I. INTRODUCTION

Supersymmetry (SUSY) is one of the most promising extensions of the standard model (SM). Not only does it provide a natural solution to the gauge hierarchy problem, but also gives a dynamical mechanism for electroweak symmetry breaking and a natural candidate for the dark matter. The simplest and most popular realization of supersymmetry is the minimal supersymmetric standard model (MSSM) [1, 2, 3]. The MSSM predicts the existence of scalar partners to all known quarks and leptons, via which the electroweak scale is stabilized. Since none of these SUSY partners have been found, the SUSY must be broken in our present world. Naively, we expect the SUSY particles to be heavier than their SM counter parts; however, naturalness arguments suggest that the scale of SUSY breaking, and hence the masses of the SUSY particles should not exceed  $\mathcal{O}(1\text{TeV})$ .

There exist some lower mass limits on these scalar SUSY partners. One of them comes from the direct search at the Tevatron. Current lower limits on the first- and second- squark masses are 200 – 300 GeV, depending on the gluino mass and the neutralino mass. An indirect limit comes from the Higgs mass bound of 114.4 GeV [4]. It is well-known in the MSSM that radiative corrections can lift the Higgs mass at its tree-level bound ( $m_Z$ ) to the current mass bound or more [5]. The major correction comes from the top-stop loop. The current Higgs mass bound demands either (i) the top squark mass to be of order 1 TeV, or (ii) the mixing between the left- and right-handed top squark to be strong. While the first condition makes the search at the LHC experiments very difficult, the second option becomes very interesting. Not only can it satisfy the Higgs mass bound, but also allow a relatively light top squark as light as 200 GeV, which can certainly be produced at the LHC or may be even at the Tevatron. The left-right mixing effect in the first two generations of squark is negligible. Furthermore, the third generation of scalar fermions,  $\tilde{t}$ ,  $\tilde{b}$ , and  $\tilde{\tau}$  are expected to be lighter than the corresponding scalar fermions of the first and second generations in Grand Unified SUSY models, because of the large Yukawa-coupling evolution. Therefore, potentially the top and bottom squarks are among the first SUSY particles to be discovered at the LHC. In this work, we focus on the third generation squark-pair production.

There have been many works on hadronic production of top and bottom squarks [6]. The leading order (LO) cross section for diagonal top-squark pair production  $\tilde{t}_i\tilde{t}_i$  ( $i=1,2$ ) via gg scattering in hadron collisions was first calculated in Ref. [7]. However, these scattering reactions only lead to squark and antisquark pairs of the same flavor and same mass eigenstates, i.e.,  $\tilde{t}_1\tilde{t}_1^*$ ,  $\tilde{t}_2\tilde{t}_2^*$ , not only because gluons do not couple to  $\tilde{t}_L\tilde{t}_R^*$  pair, but also because the coupling strengths to  $LL$  and  $RR$  are the same. Furthermore, such squark-pair production via QCD is weakly dependent of  $\tan\beta$ . The next-to-leading order (NLO) calculations have been improved by a number of authors [8, 9], including SUSY-QCD corrections. Recently, NLO electroweak contribution of  $\mathcal{O}(\alpha_s^2\alpha)$  as well as the lowest-order  $\mathcal{O}(\alpha_s\alpha+\alpha^2)$  electroweak terms to the production of diagonal squarks were studied and shown to be sizable [10]. It was shown in Ref. [11] that the tree level electroweak contributions to the production of squark pairs at hadron colliders, which includes s-channel gauge boson exchanges as well as t and/or u channel gaugino exchanges, are comparable to the dominant QCD contributions in some cases. Note that in that study [11] the  $b\bar{b}$  initial-state contribution was not included.

Non-diagonal squark-pair production, like  $\tilde{t}_1\tilde{t}_2^*$  and  $\tilde{b}_1\tilde{b}_2^*$ , is possible at tree level via  $Z$  boson exchange, as the  $LL$  and  $RR$  couplings are different [12]. Mixed top and bottom squark production  $\tilde{t}_i\tilde{b}_j^*$  is also possible via an intermediate  $W$  boson in the  $2 \rightarrow 2$  subprocess or via  $gW$  fusion in the  $2 \rightarrow 3$  subprocess [12]. All these non-diagonal  $\tilde{t}_i\tilde{t}_j^*$ ,  $\tilde{t}_i\tilde{b}_j^*$ , and  $\tilde{b}_i\tilde{b}_j^*$

pairs with  $i \neq j$  are produced via exchanges of electroweak gauge bosons, and therefore the production rates are smaller than the corresponding diagonal pairs.

In this work, we point out that the  $s$ -channel exchange of various Higgs bosons plays an important role here, namely, it can substantially enhance the production rate, especially at large  $\tan \beta$ . In this paper, we investigate the importance of electroweak channels including the neutral Higgs bosons for  $\tilde{t}_i \tilde{t}_j^*$  and  $\tilde{b}_i \tilde{b}_j^*$  pair production and charged Higgs boson for  $\tilde{t}_i \tilde{b}_j^*$  pair at hadron colliders when one or both of the initial-state partons are the bottom quark. We anticipate the contributions from the Higgs exchanges will be substantial at large  $\tan \beta$  region, where the smallness of the bottom-parton luminosity can be compensated by enhancement of the bottom Yukawa coupling.

Furthermore, it also allows resonant Higgs production for relatively heavy Higgs bosons  $H^\pm$ ,  $H^0$ , and  $A^0$ . In fact, with  $m_{H^0, A^0, H^\pm} > m_{\tilde{q}_i} + m_{\tilde{q}_j}$ , the nondiagonal squark pair production offers an interesting possibility to study the squark-squark-Higgs couplings right at the Higgs boson resonances. In addition, with the intermediate charged Higgs boson all left- and right-handed squark pairs  $\tilde{t}_{L,R} \tilde{b}_{L,R}$  can be produced while only  $\tilde{t}_L \tilde{b}_L$  can be produced via the intermediate  $W$  exchange. Thus, we anticipate the production via intermediate charged Higgs boson could be dominant in some region of parameter space. We explore the MSSM parameter space relevant for our study.

The organization is as follows. In the next section, we will write the details of the couplings and mass matrices. In Sec. III, we describe the formulas for squark-pair production. In Sec. IV, we discuss the effect of phenomenological constraints on SUSY parameters, followed by numerical results on production cross sections. We conclude in Sec. V.

## II. FORMALISM

We start with the following superpotential

$$W = \epsilon_{ab} [y_{ij}^u Q_j^a H_u^b U_i^c - y_{ij}^d Q_j^a H_d^b D_i^c - y_{ij}^l L_j^a H_d^b E_i^c + \mu H_u^a H_d^b] , \quad (1)$$

where  $\epsilon_{12} = -\epsilon_{21} = 1$ ,  $i, j$  are family indices, and  $y^u$  and  $y^d$  represent the Yukawa matrices for the up-type and down-type quarks, respectively. Here  $Q, L, U^c, D^c, E^c, H_u$ , and  $H_d$  denote the quark doublet, lepton doublet, up-type quark singlet, down-type quark singlet, lepton singlet, up-type Higgs doublet, and down-type Higgs doublet superfields, respectively.

### A. Quark mass matrices

The Higgs doublets develop vacuum expectation values (VEV), which break the electroweak symmetry, are

$$\langle H_u \rangle = \frac{1}{\sqrt{2}} \begin{pmatrix} 0 \\ v \sin \beta \end{pmatrix} , \quad \text{and} \quad \langle H_d \rangle = \frac{1}{\sqrt{2}} \begin{pmatrix} v \cos \beta \\ 0 \end{pmatrix} , \quad (2)$$

where  $v \approx 246$  GeV, and the quark mass terms are given by

$$\mathcal{L}_{\text{quark}} = -y_{ij}^u \frac{v \sin \beta}{\sqrt{2}} \bar{u}_{Ri} u_{Lj} - y_{ij}^d \frac{v \cos \beta}{\sqrt{2}} \bar{d}_{Ri} d_{Lj} + \text{h.c.} . \quad (3)$$

The Yukawa matrices  $y^u$  and  $y^d$  are diagonalized by bi-unitary transformations:

$$\begin{pmatrix} d_1 \\ d_2 \\ d_3 \end{pmatrix}_{L,R} = D_{L,R} \begin{pmatrix} d \\ s \\ b \end{pmatrix}_{L,R}, \quad \begin{pmatrix} u_1 \\ u_2 \\ u_3 \end{pmatrix}_{L,R} = U_{L,R} \begin{pmatrix} u \\ c \\ t \end{pmatrix}_{L,R}, \quad (4)$$

and

$$U_R^\dagger \left( y^u \frac{v \sin \beta}{\sqrt{2}} \right) U_L = \begin{pmatrix} m_u & 0 & 0 \\ 0 & m_c & 0 \\ 0 & 0 & m_t \end{pmatrix}, \quad D_R^\dagger \left( y^d \frac{v \cos \beta}{\sqrt{2}} \right) D_L = \begin{pmatrix} m_d & 0 & 0 \\ 0 & m_s & 0 \\ 0 & 0 & m_b \end{pmatrix}. \quad (5)$$

We define the diagonal Yukawa matrices  $Y^u$  and  $Y^d$  as

$$Y^u = \frac{\sqrt{2}}{v \sin \beta} \begin{pmatrix} m_u & 0 & 0 \\ 0 & m_c & 0 \\ 0 & 0 & m_t \end{pmatrix}, \quad Y^d = \frac{\sqrt{2}}{v \cos \beta} \begin{pmatrix} m_d & 0 & 0 \\ 0 & m_s & 0 \\ 0 & 0 & m_b \end{pmatrix}. \quad (6)$$

In order to avoid excessive flavor-changing neutral currents, we assume that the squark mass matrices are in alignment with the quark mass matrices, i.e., they are diagonalized by the same bi-unitary transformations:

$$\begin{pmatrix} \tilde{u}_1 \\ \tilde{u}_2 \\ \tilde{u}_3 \end{pmatrix}_{L,R} = U_{L,R} \begin{pmatrix} \tilde{u} \\ \tilde{c} \\ \tilde{t} \end{pmatrix}_{L,R}, \quad \begin{pmatrix} \tilde{d}_1 \\ \tilde{d}_2 \\ \tilde{d}_3 \end{pmatrix}_{L,R} = D_{L,R} \begin{pmatrix} \tilde{d} \\ \tilde{s} \\ \tilde{b} \end{pmatrix}_{L,R}, \quad (7)$$

Here  $d_1, d_2, d_3$  are in interaction basis while  $d, s, b$  are in mass eigenbasis. Without loss of generality, we can make the choice that the right-handed quarks and squarks are already in the mass eigenbasis, i.e.,  $D_R = U_R = I$ . The information on the left-handed unitary matrices  $D_L, U_L$  is encoded in the Kobayashi-Maskawa (KM) matrix as

$$V_{KM} = U_L^\dagger D_L. \quad (8)$$

## B. Squark mass matrices

Even after we have rotated the quark and squark mass matrices into family-diagonal form with the same bi-unitary transformation, within one family the left-handed and right-handed squarks will mix due to the soft terms and  $F$  terms in the Lagrangian. This  $LR$  mixing is proportional to the quark mass concerned such that the  $LR$  mixing for the first two generations are negligible while it can be substantial for the third generation. From now on we only concern the  $LR$  squark mixing in the third generation.

The squark mass-squared matrix in the  $L$ - $R$  basis have the form

$$\mathcal{M}_{\tilde{q}}^2 = \begin{pmatrix} m_{LL}^2 & m_{LR}^2 \\ m_{LR}^{2*} & m_{RR}^2 \end{pmatrix} \quad (9)$$

with

$$m_{LL}^2 = \widetilde{M}_L^2 + m_q^2 + m_Z^2 \cos 2\beta (I_3^q - e_q s_W^2), \quad (10)$$

$$m_{RR}^2 = \widetilde{M}_R^2 + m_q^2 + m_Z^2 \cos 2\beta e_q s_W^2, \quad (11)$$

$$m_{LR}^2 = m_q \left[ A_q^* - \mu (\tan \beta)^{-2I_3^q} \right], \quad (12)$$

where  $I_3^q = \pm 1/2$  and  $e_q$  are the third component of the weak isospin and the electric charge of the quark  $q$ . In Eqs. (9),  $\mu$  is the supersymmetric Higgs mass parameter,  $\widetilde{M}_L^2$  the soft-breaking mass parameter for the squark iso-doublet  $(\widetilde{q}_L, \widetilde{q}'_L)$ , and  $\widetilde{M}_R^2$  are the soft-breaking mass parameters for the iso-singlets  $\widetilde{q}_R$ . They can be different for each generation, but for simplicity we will assume equal values for all generations  $\widetilde{M}_L = \widetilde{M}_R = M_{SUSY}$  in our numerical analysis.  $A_q$  are the parameters of the soft-breaking scalar three-point interactions of top- and bottom-squarks with the Higgs fields.

The hermitian matrix in Eq. (9) is diagonalized by a unitarity matrix  $R^{\widetilde{q}}$ , which rotates the current eigenstates,  $\widetilde{q}_L$  and  $\widetilde{q}_R$ , into the mass eigenstates  $\widetilde{q}_1$  and  $\widetilde{q}_2$  as follows,

$$\begin{pmatrix} \widetilde{q}_1 \\ \widetilde{q}_2 \end{pmatrix} = R^{\widetilde{q}} \begin{pmatrix} \widetilde{q}_L \\ \widetilde{q}_R \end{pmatrix} = \underbrace{\begin{pmatrix} \cos \widetilde{\theta}_q & \sin \widetilde{\theta}_q \\ -\sin \theta_q & \cos \theta_q \end{pmatrix}}_{R^{\widetilde{q}}} \begin{pmatrix} \widetilde{q}_L \\ \widetilde{q}_R \end{pmatrix}, \quad (13)$$

yielding the physical mass eigenvalues, with the convention  $m_{\widetilde{q}_1} < m_{\widetilde{q}_2}$ ,

$$m_{\widetilde{q}_{1,2}}^2 = \frac{1}{2} \left( m_{LL}^2 + m_{RR}^2 \mp \sqrt{(m_{LL}^2 - m_{RR}^2)^2 + 4|m_{LR}^2|^2} \right). \quad (14)$$

The mixing angle  $\widetilde{\theta}_q$  obeys the relation

$$\tan 2\widetilde{\theta}_q = \frac{2m_{LR}^2}{m_{LL}^2 - m_{RR}^2}. \quad (15)$$

Hence, for the case of the supersymmetric partners of the light fermions,  $L$ - $R$  mixing can be neglected. However, mixing between top squarks can be sizable and allows one of the two mass eigenstates to be lighter than the top quark. Bottom-squark mixing can also be significant if  $\tan \beta$  is large.

### C. Higgs and gauge bosons interactions with quarks and squarks

Let  $H_k = (h^0, H^0, A^0, G^0)$  ( $k=1\dots 4$ ), one can write the relevant Lagrangian density in the  $(\widetilde{q}_1, \widetilde{q}_2)$  basis as following form ( $i, j=1,2$ )

$$\begin{aligned} \mathcal{L}_{\text{relevant}} &= g_{H_k qq} H_k \bar{q} q + (G_k)_{ij} H_k \widetilde{q}_j^* \widetilde{q}_i + (G_5)_{ij} H^+ \widetilde{q}_j^* \widetilde{q}_i \\ &+ g\bar{q}(\mathcal{A}_{im}^{\widetilde{q}} P_R + \mathcal{B}_{im}^{\widetilde{q}}) \widetilde{\chi}_m^0 \widetilde{q}_i + g\bar{q}'(\mathcal{L}_{il}^{\widetilde{q}} P_R + \mathcal{K}_{il}^{\widetilde{q}} P_L) \widetilde{\chi}_l^{+c} \widetilde{q}_i \\ &+ H^+ \bar{u} (Y^u \cos \beta P_L + Y^d \sin \beta P_R) V_{KM} d \\ &+ G^+ \bar{u} (Y^u \sin \beta P_L - Y^d \cos \beta P_R) V_{KM} d \\ &+ \text{h.c} \end{aligned} \quad (16)$$

The Feynman rules are  $ig_{H_k qq}$  for  $k=1,2$  and  $\gamma_5 g_{H_k qq}$  for  $k=3,4$  where we list only Higgs bosons couplings to quark  $b$ , and

$$g_{hbb} = \frac{g m_b \sin \alpha}{2m_W \cos \beta}, \quad g_{Hbb} = -\frac{g m_b \cos \alpha}{2m_W \cos \beta}, \quad g_{Abb} = -\frac{g m_b}{2m_W} \tan \beta. \quad (17)$$

The couplings  $G_k$  and  $G_5$  are given in the mass basis by

$$G_k = \mathcal{R}^{\tilde{q}} \hat{G}_k (\mathcal{R}^{\tilde{q}})^T, \quad (k = 1 \dots 4), \quad G_5 = \mathcal{R}^{\tilde{t}} \hat{G}_5 (\mathcal{R}^{\tilde{b}})^T \quad (18)$$

where  $\hat{G}_k$  and  $\hat{G}_5$  are the couplings in the  $(\tilde{q}_L, \tilde{q}_R)$  basis, and their explicit forms are shown in Appendix A. Finally,  $\mathcal{A}_{im}^{\tilde{q}}$ ,  $\mathcal{B}_{im}^{\tilde{q}}$  ( $m=1 \dots 4$ ), and  $\mathcal{L}_{il}^{\tilde{q}}$ ,  $\mathcal{K}_{il}^{\tilde{q}}$  ( $l=1,2$ ) used in Eq.(16) are defined also in the end of Appendix A.

The  $W$  and  $Z$  bosons interactions with the quarks are given by

$$\mathcal{L} = -\frac{g}{\sqrt{2}} \bar{u} \gamma^\mu V_{KM} P_L d W_\mu^+ - g Z \bar{q} \gamma^\mu (C_{qL} P_L + C_{qR} P_R) q + \text{H.c.} \quad (19)$$

with

$$C_{qL,R} = \frac{1}{\cos \theta_W} (I_{3L,R}^q - e_q \sin^2 \theta_W) \quad (20)$$

The  $W$  and  $Z$  bosons interactions with the squarks are given by

$$\mathcal{L} = -i g g_{W\tilde{q}_i\tilde{q}_j} W_\mu^+ \tilde{u}_j^* \overset{\leftrightarrow}{\partial}^\mu \tilde{d}_i - i g g_{Z\tilde{q}_i\tilde{q}_j} Z \tilde{q}_i^* \overset{\leftrightarrow}{\partial}^\mu \tilde{q}_j + \text{h.c.} \quad (21)$$

with

$$g_{W\tilde{q}_i\tilde{q}_j} = \frac{1}{\sqrt{2}} \begin{pmatrix} \cos \theta_{\tilde{u}} \cos \theta_{\tilde{d}} & -\cos \theta_{\tilde{u}} \sin \theta_{\tilde{d}} \\ -\sin \theta_{\tilde{u}} \cos \theta_{\tilde{d}} & \sin \theta_{\tilde{u}} \sin \theta_{\tilde{d}} \end{pmatrix}_{ij} \quad (22)$$

and

$$g_{Z\tilde{q}_i\tilde{q}_j} = \frac{1}{\cos \theta_W} \begin{pmatrix} I_{3L}^q \cos^2 \theta_{\tilde{q}} - e_q \sin^2 \theta_W & -\frac{1}{2} I_{3L}^q \sin 2\theta_{\tilde{q}} \\ -\frac{1}{2} I_{3L}^q \sin 2\theta_{\tilde{q}} & I_{3L}^q \sin^2 \theta_{\tilde{q}} - e_q \sin^2 \theta_W \end{pmatrix}_{ij} \quad (23)$$

#### D. Radiative corrections to the Yukawa couplings

Note that both initial and final states have the bottom Yukawa  $Y^b$  dependence. It is now well established that the coupling of the scalar bottom  $\tilde{b}$  to the up-type Higgs doublet induces a modification of the tree-level relation between the bottom quark mass and its Yukawa coupling [19, 20, 21, 22]. Those corrections are amplified at large  $\tan \beta$ . The modifications can be absorbed by redefining the bottom Yukawa coupling as [19, 20, 21, 22]

$$Y^b = \frac{\sqrt{2} m_b}{v \cos \beta} \rightarrow \frac{\sqrt{2}}{v \cos \beta} \frac{m_b}{1 + \Delta_b} \approx \frac{\sqrt{2}}{v} \frac{m_b}{1 + \Delta_b} \tan \beta \quad (24)$$

where the second term is valid for large  $\tan \beta$  and the SUSY-QCD corrections lead to

$$\Delta_b = \frac{2\alpha_s}{3\pi} \mu m_{\tilde{g}} \tan \beta I(m_{\tilde{b}_1}, m_{\tilde{b}_2}, m_{\tilde{g}}) + \frac{(Y^t)^2}{16\pi^2} \mu A_t \tan \beta I(m_{\tilde{t}_1}, m_{\tilde{t}_2}, \mu) \quad (25)$$

where  $m_{\tilde{g}}$  is the gluino mass, and the function  $I$  is given by

$$I(a, b, c) = \frac{1}{(a^2 - b^2)(b^2 - c^2)(a^2 - c^2)} (a^2 b^2 \ln \frac{a^2}{b^2} + b^2 c^2 \ln \frac{b^2}{c^2} + c^2 a^2 \ln \frac{c^2}{a^2}) \quad . \quad (26)$$

In  $\Delta_b$  we only keep the dominant contributions from the gluino-sbottom and charged-higgsino-stop loops because they are proportional to the strong coupling and to the top Yukawa coupling, respectively, while neglecting those that are proportional to the weak gauge coupling. Note that  $\Delta_b$  is evaluated at the scale of SUSY particles  $M_{\text{susy}}$ , where the heavy particles in the loop decouple, whereas the bottom Yukawa coupling  $Y^b(Q)$  at any scale  $Q$  is determined by the running  $b$ -quark mass  $m_b(Q)$  at the scale  $Q$ :

The contributions to the bottom Yukawa couplings which are enhanced at large  $\tan\beta$  can be included to all orders by making the following replacements [19, 20, 23, 24]

$$g_{hbb} \rightarrow g_{hbb} \frac{1 - \Delta_b / (\tan\beta \tan\alpha)}{1 + \Delta_b} \quad (27)$$

$$g_{Hbb} \rightarrow g_{Hbb} \frac{1 + \Delta_b \tan\alpha / \tan\beta}{1 + \Delta_b} \quad (28)$$

$$g_{Abb} \rightarrow g_{Abb} \frac{1 - \Delta_b / \tan^2\beta}{1 + \Delta_b} \quad (29)$$

$$Y^b \rightarrow \frac{\sqrt{2}m_b(Q)}{v \cos\beta} \frac{1}{1 + \Delta_b} \quad (30)$$

We now have all the tools to compute the production cross section of sbottom and stop.

### III. SQUARK PAIR PRODUCTION

In this section we discuss squark-pair production. Let us define our notation for the convenience of the following formulas. The momenta of the incoming quark  $q$  and anti-quark  $\bar{q}$ , outgoing squark  $\tilde{q}_i$  and outgoing anti-squark  $\tilde{q}_j^*$  are denoted by  $p_1$ ,  $p_2$ ,  $k_1$  and  $k_2$ , respectively. We neglect the quark masses of the incoming partons. The Mandelstam variables are defined as follows

$$\begin{aligned} \hat{s} &= (p_1 + p_2)^2 = (k_1 + k_2)^2 \\ \hat{t} &= (p_1 - k_1)^2 = (p_2 - k_2)^2 = \frac{m_{\tilde{q}_i}^2 + m_{\tilde{q}_j}^2}{2} - \frac{\hat{s}}{2} (1 - \beta \cos\theta^*) \\ \hat{u} &= (p_1 - k_2)^2 = (p_2 - k_1)^2 = \frac{m_{\tilde{q}_i}^2 + m_{\tilde{q}_j}^2}{2} - \frac{\hat{s}}{2} (1 + \beta \cos\theta^*) \end{aligned} \quad (31)$$

where  $\beta = \lambda^{1/2}(1, m_{\tilde{q}_i}^2/\hat{s}, m_{\tilde{q}_j}^2/\hat{s})$  and  $\theta^*$  is the scattering angle in the center-of-mass frame of the partons.

#### A. Hadronic production of $q\bar{q}, gg \rightarrow \tilde{t}_i\tilde{t}_j^*, \tilde{b}_i\tilde{b}_j^*$

The production of top and bottom squark pair proceeds via the following  $q\bar{q}$ - and  $gg$ -initiated subprocesses which are depicted in Fig. 1(a) – (h).

$$q\bar{q}, gg \rightarrow \tilde{t}_i\tilde{t}_j^*, \tilde{b}_i\tilde{b}_j^*, \quad (32)$$

where  $(i, j) = (1, 2)$ .

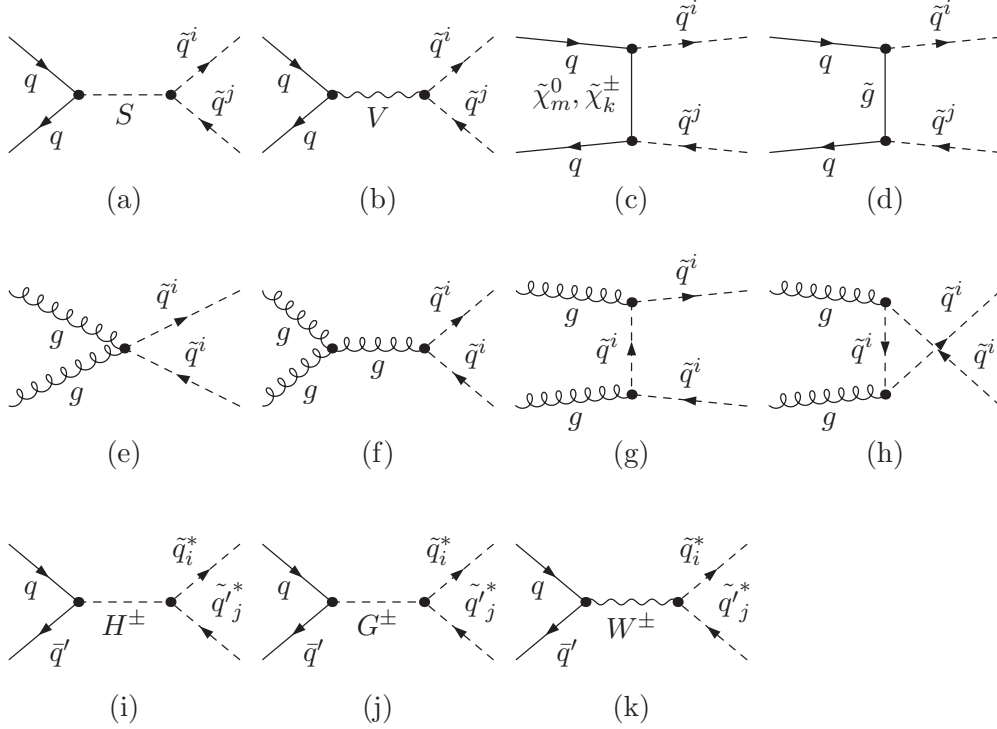


FIG. 1: Tree-level Feynman diagrams for squarks pair production via  $q\bar{q}$ ,  $gg$ , and  $q\bar{q}'$  annihilation. With  $(i,j) = (1,2)$ ,  $q = (u, d, c, s, b)$ ,  $S = h^0, H^0, A^0, G^0$  and  $V = \gamma, Z, g$ . In diagram (b), the photon and gluon do not contribute to non-diagonal production.

Note that the photon and gluon do not contribute to production of  $\tilde{q}_1\tilde{q}_2^*$ , because of electromagnetic or color conservation. Consequently, at tree level the above reactions proceed only through s-channel Z boson and Higgs bosons. If the initial state is  $u\bar{u}$ ,  $d\bar{d}$ ,  $s\bar{s}$  or  $c\bar{c}$ , the Yukawa couplings are so small that we consider only the contribution from the Z exchange diagram. While in the case of  $b\bar{b}$ , the cross section will directly determined by the size of Higgs coupling to a squarks  $S\tilde{q}_1\tilde{q}_2$  where  $S = h^0, H^0$  or  $A^0$  and  $Z\tilde{q}_1\tilde{q}_2$  couplings, which are proportional to  $\sin 2\theta_{\tilde{q}}$  of the squark-mixing angle  $\theta_{\tilde{q}}$ . therefore, these processes can be used to probe the mixing angle  $\theta_{\tilde{q}}$ . The analytic expressions for  $b\bar{b} \rightarrow \tilde{t}_i\tilde{t}_j^*$  and  $b\bar{b} \rightarrow \tilde{b}_i\tilde{b}_j^*$  are given in appendix B.

The gluon-gluon fusion into  $\tilde{t}_1\tilde{t}_2^*$  and  $\tilde{b}_1\tilde{b}_2^*$  only goes through loop diagrams, as shown in Fig. 2. These one loop contributions are of the order of either  $\alpha_s^2$  or  $\alpha_s\alpha$ .

The hadronic inclusive cross section for  $\tilde{q}_i\tilde{q}_j^*$  production in proton-proton collisions at a total hadronic center of mass energy  $\sqrt{S}$  can be written as [29]

$$\sigma_{pp \rightarrow \tilde{q}_i\tilde{q}_j^*}(S) = \sum_q \int_{\tau_0}^1 d\tau \frac{d\mathcal{L}_{q\bar{q}}^{pp}}{d\tau} \hat{\sigma}_{LO}(q\bar{q} \rightarrow \tilde{q}_i\tilde{q}_j^*)(\tau S) + \int_{\tau_0}^1 d\tau \frac{d\mathcal{L}_{gg}^{pp}}{d\tau} \hat{\sigma}_{LO}(gg \rightarrow \tilde{q}_i\tilde{q}_j^*)(\tau S) \quad (33)$$

where  $\tau_0 = (m_{\tilde{q}_i}^2 + m_{\tilde{q}_j}^2)/S$ , and the parton luminosity is

$$\frac{d\mathcal{L}_{ab}^{pp}}{d\tau} = \int_{\tau}^1 \frac{dx}{x} \frac{1}{1 + \delta_{ab}} [f_a(x, \mu_F) f_b(\frac{\tau}{x}, \mu_F) + f_b(x, \mu_F) f_a(\frac{\tau}{x}, \mu_F)] \quad (34)$$

where  $f_a(x, \mu_F)$  is parton distribution functions (PDF) for each type  $a$  in the proton carrying a fraction  $x$  of the proton momentum at scale  $\mu_F = m_{\tilde{q}_i} + m_{\tilde{q}_j}$ .



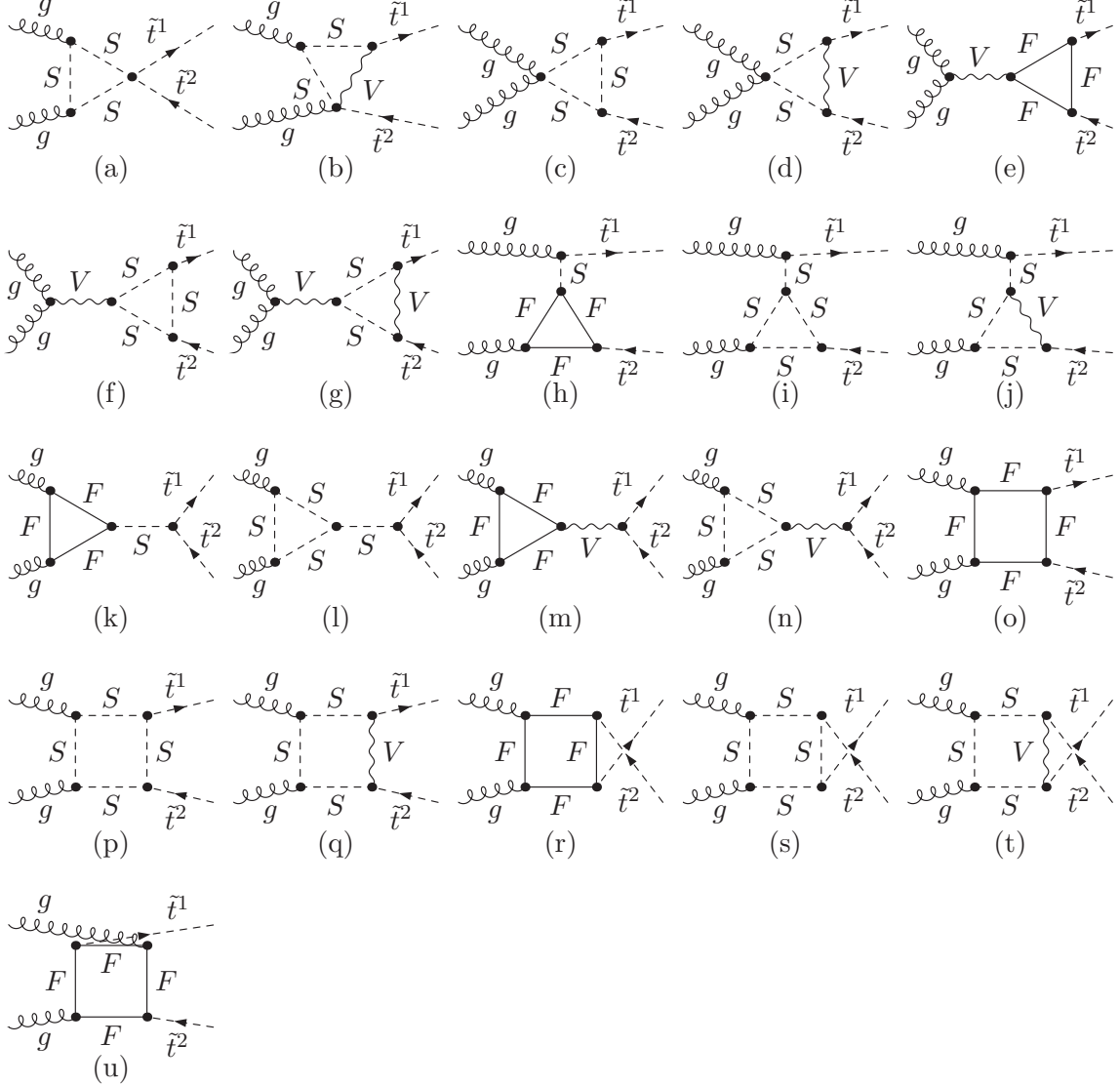


FIG. 2: One-loop Feynman diagrams for squark-pair production in gluon-gluon fusion. With  $i \neq j = (1,2)$ ,  $F = \tilde{g}, \tilde{\chi}^0, \tilde{\chi}^\pm$ ,  $S = h^0, H^0, A^0, G^0$  and  $V = \gamma, Z, g$ .

### B. Hadronic production of $d\bar{u} \rightarrow \tilde{t}_i \tilde{b}_j^*$

In this case, the Mandelstam variables are defined as in Eq. (31) with  $m_{\tilde{q}_i} = m_{\tilde{t}_i}$  and  $m_{\tilde{q}_j} = m_{\tilde{b}_j}$ . At hadron colliders, the production mechanism proceeds via the conventional Drell-Yan processes with the charged Higgs boson, charged Goldstone and charged gauge bosons, as depicted in Fig. 1 (i)-(k). The  $s$ -channel diagram with charged Higgs exchange

dominates when  $\sqrt{\hat{s}}$  is close to  $M_{H^\pm}$ . The analytic expressions for the cross sections are given in appendix B.

## IV. NUMERICAL RESULTS

### A. Phenomenological constraints

In this section, and before presenting our numerical results, we would like to list the phenomenological constraints included when determining the allowed parameter space [13, 14].

- The most stringent constraint generally arises from  $\Delta\rho^{SUSY}$  which receives contributions from both stop and sbottom. The extra contributions to the  $\Delta\rho^{SUSY}$  parameter from the stop and sbottom sector [15, 16] should not exceed the current limit from precision measurements [17]:  $\Delta\rho^{SUSY} \leq 10^{-3}$ .
- The soft SUSY-breaking parameters  $A_q$  at the weak scale should not be too large in order to keep the radiative corrections to the Higgs masses under control. In particular the trilinear couplings of the third generation squarks  $A_{t,b}$ , they will play a particularly important role in the MSSM squarks/Higgs sectors. These parameters can be constrained in at least one way, besides the trivial requirement that it should not make the off-diagonal term of the squark mass matrices too large to generate too low masses for the squarks.  $A_{t,b}$  should not be too large to avoid the occurrence of charge and color breaking (CCB) minima in the Higgs potential. To avoid such minima at tree level,  $A_{t,b}$  have to satisfy the following tree level conditions[18].

$$A_t^2 \leq 3(m_{\tilde{t}_2}^2 + m_{\tilde{t}_1}^2 - 2m_t^2 + \frac{1}{2}m_Z^2 \cos 2\beta + M_{H_2}^2 + \mu^2), \quad (35)$$

$$A_b^2 \leq 3(m_{\tilde{b}_2}^2 + m_{\tilde{b}_1}^2 - 2m_b^2 + \frac{1}{2}m_Z^2 \cos 2\beta + M_{H_1}^2 + \mu^2). \quad (36)$$

With  $M_{H_1}^2 = (m_{A^0}^2 + m_Z^2) \sin^2 \beta - 1/2m_Z^2$  and  $M_{H_1}^2 + M_{H_2}^2 = m_{A^0}^2$ . The above constraints depend on  $\mu$  and  $A_{t,b}$  explicitly.

- Another constraint which has been imposed is the perturbativity of the bottom Yukawa coupling. Since radiative corrections to the bottom Yukawa coupling have been implemented as in Eq. (30), the Yukawa may blow up when SUSY parameters varies. Thus, we restrict  $Y^b \lesssim (4\pi)^2$ .
- We have imposed also all the experimental bounds on squark, chargino, and neutralino masses as well as Higgs boson masses [17].

### B. Numerical results

In this section, we present the numerical result for inclusive production cross section of diagonal, non-diagonal and mixed squarks at the LHC with a proton-proton center-of-mass energy cross sections of 14 TeV. In our numerical calculations the following SM input

parameters were chosen [17]:

$$\begin{aligned} m_t &= 171.9 \text{ GeV} \quad , \quad m_W = 80.398 \text{ GeV} \quad , \quad m_Z = 91.1878 \text{ GeV} \\ G_F &= 1.16637 \times 10^{-5} \text{ GeV}^{-2} \quad , \quad V_{cb} = 0.04, \quad m_b(m_b) = 4.25 \text{ GeV} \end{aligned} \quad (37)$$

The running QCD coupling  $\alpha_s$  was evaluated at the two-loop level [25] and the CTEQ6L PDFs [28, 29] were used to calculate the various cross sections. Moreover, in order to improve the perturbative calculations, 1-loop running masses  $m_b(Q)$  were taken as following:

$$m_b(Q) = m_b^{\overline{\text{DR}}}(Q) = m_b^{\overline{\text{MS}}}(Q) \left( 1 + \frac{4\alpha_s}{3\pi} \right) \quad (38)$$

where  $m_b^{\overline{\text{MS}}}$  includes the SM QCD corrections.

First of all, we investigate the effect of varying the MSSM parameters for which the correction to  $\Delta_b$  term are expected to have a large impact. In the limit where the squark and gluino masses have approximately the same value, denoted by the common SUSY mass  $M_{SUSY}$ , the Eq. (26) simplifies to

$$I(m_{SUSY}, m_{SUSY}, m_{SUSY}) = \frac{1}{2m_{SUSY}^2}. \quad (39)$$

Furthermore, if  $\mu$  is of similar size, the first term in Eq. (25) is dominant and reduces to

$$\Delta_b \approx \text{sign}(\mu) \frac{\alpha_s}{3\pi} \tan \beta \quad (40)$$

So, for large  $\tan \beta$  this effect can be  $\mathcal{O}(1)$  and does not vanish for a heavy SUSY spectrum. The sign of  $\mu$  is the decisive factor in determining whether the corrections will enhance or suppress the cross section for the processes of  $pp \rightarrow b\bar{b} \rightarrow \tilde{b}_i \tilde{b}_j^*, \tilde{t}_i \tilde{t}_j^*, \tilde{t}_i \tilde{b}_j^*$ . We assume the universality of soft SUSY breaking trilinear couplings:  $A_t = A_b = A_\tau = A_0$ . We parameterize the squark sector using the following input parameters:  $\tan \beta$ ,  $\mu$ ,  $A_0$  and the gluino mass  $m_{\tilde{g}}$ . The MSSM Higgs sector is parameterized by the mass of CP-odd  $m_{A^0}$  and  $\tan \beta$  as well as by  $M_{SUSY}$ ,  $A_{b,t}$  and  $\mu$  for higher order corrections [26, 27]. All the MSSM Higgs masses and parameters are computed with FeynHiggs code [26].

We present the results of diagonal squark production of  $\tilde{b}_1 \tilde{b}_1^*$  in Fig. 3 and  $\tilde{t}_1 \tilde{t}_1^*$  in Fig. 4, respectively. At the LHC, the diagonal pair production of  $\tilde{t}_1 \tilde{t}_1^*$  and  $\tilde{b}_1 \tilde{b}_1^*$  is dominated by  $gg$  fusion. However, it is noted that the  $b\bar{b}$ -initiated subprocess already surpass the light  $q\bar{q}$ -initiated channels when  $\tan \beta \gtrsim 17$ , because of the enhancement from the Higgs boson couplings to the bottom quark as well as from the large coupling of Higgs to a pair of squarks.

The cross sections  $\sigma(b\bar{b}, gg, \sum q\bar{q} \rightarrow \tilde{t}_1 \tilde{t}_1^* \text{ and } \tilde{b}_1 \tilde{b}_1^*)$  are plotted as a function of pseudoscalar Higgs mass  $m_{A^0}$  for a large  $\tan \beta$  in the right panel and as a function of  $\tan \beta$  at around the resonance  $m_{A^0} \approx 2m_{\tilde{q}}$ , where  $q = b, t$ , in the left panel. The size of these cross sections depend strongly on the Higgs mass and  $\tan \beta$ . We note that indeed the leading order cross section  $\sigma(b\bar{b} \rightarrow \tilde{t}_1 \tilde{t}_1^* \text{ and } \tilde{b}_1 \tilde{b}_1^*)$  increases like  $\tan^2 \beta$  for large values of  $\tan \beta$ . To understand this we separate various contributions to the production rate. The bottom-induced Drell-Yan contribution proceeds through an s-channel photon or Z boson. The coupling to the photon is independent of  $\tan \beta$  and the dependence of the Z couplings is small for large enough values of the pseudoscalar Higgs mass. A second set of s-channel production processes is made possible by the incoming bottom quarks and their finite Yukawa couplings to CP-even Higgs bosons  $h^0, H^0$ , but the CP-odd pseudoscalar exchange is forbidden by the CP

symmetry of the final state. The couplings  $h^0\tilde{b}_1\tilde{b}_1$  and  $H^0\tilde{b}_1\tilde{b}_1$  depend strongly on  $\tan\beta$  and on other MSSM parameters such as  $\mu$  and soft trilinear terms  $A_{t,b}$ . Note that the dependence on  $\tan\beta$  and  $\mu$  parameter also comes in through  $\Delta_b$  corrections.

The relative size of the Higgs contribution compared to Drell-Yan process show up at large  $\tan\beta$  and near the resonance. Note that the interference between Higgs contributions and the QCD are zero due to color structure. The process  $b\bar{b} \rightarrow \tilde{q}_1\tilde{q}_1^*$  receives EW contributions from t-channel exchange of a neutralino and gluino if  $q = b$  and chargino exchange contribution if  $q = t$ . The corresponding Feynman diagrams are shown in Fig. 1(c) and (d). Combining s-channel and t-channel including Higgs contributions, we see that they interfere constructively. Since QCD contributions dominate even after inclusion of the electroweak diagrams, the overall behavior of the total cross sections does not change much. For example, for  $\tan\beta \sim 20$ , the EW increase the cross section for the pair production of  $\tilde{b}_1\tilde{b}_1$  squarks by about 2pb, whereas they only contribute 24% to the total cross section.

In gluon-gluon fusion, the non-diagonal squark  $\tilde{q}_i\tilde{q}_j^*$  with  $i \neq j$  cannot be produced at the lowest order but via loop diagrams (see Fig. 2). The production cross section is therefore of the order  $\mathcal{O}(\alpha_s^4 + \alpha_s^2\alpha^2)$ . This higher-order cross section will be small compared to  $q\bar{q}$  tree level contribution. The  $b\bar{b}$ -fusion into non-diagonal squark pair proceeds via CP-even Higgs bosons  $h^0, H^0$ , and CP-odd Higgs boson  $A^0$  in s-channel, gluino and neutralino in t-channel for  $\tilde{b}_1\tilde{b}_2^*$  and chargino in t-channel for  $\tilde{t}_1\tilde{t}_2^*$  pair production. The cross sections  $\sigma(\tilde{b}_1\tilde{b}_2^* + \tilde{b}_2\tilde{b}_1^*)$  and  $\sigma(\tilde{t}_1\tilde{t}_2^* + \tilde{t}_2\tilde{t}_1^*)$  are plotted as a function of  $\tan\beta$  in the left panel and as a function of  $m_A$  in the right panel of Fig. 5 and Fig. 6, respectively. As we can see, the cross sections for both processes are small due to the absence of tree-level  $gg$  fusion and suppression from the phase space. For intermediate values of  $\tan\beta$  due to negative interference term between s-channel and t-channel diagrams all processes are comparable in size. For large  $\tan\beta$ ,  $\Delta_b$  effect induces a large enhancement for  $b\bar{b} \rightarrow \tilde{q}_1\tilde{q}_2^* + \tilde{q}_2\tilde{q}_1^*$  with  $q = b, t$  by an order of magnitude. The size of the  $b\bar{b}$ -initiated subprocess is already above the  $gg$  or  $q\bar{q}$ -initiated channels for  $\tan\beta > 5$ , as shown in Fig. 5 and Fig. 6. Note that in the case of  $b\bar{b} \rightarrow \tilde{b}_1\tilde{b}_2^*$ , we can see a spectacular enhancement for large  $\tan\beta$  (see Fig. 5 left). The origin of this enhancement is due to a factor of  $\tan\beta$  in the  $b\bar{b}A^0$  coupling and another factor of  $\tan\beta$  in the  $A^0\tilde{b}_1\tilde{b}_2^*$  coupling, which results in  $\tan^4\beta$  enhancement in cross section. This is a very interesting result that we cannot ignore the  $b\bar{b}$ -initiated subprocess with s-channel Higgs boson exchange.

Table I shows the cross sections including QCD, EW and Higgs effects. It is clear that Higgs effects enhance the cross sections for negative  $\mu$  by one to two orders of magnitudes. While they reduce the cross sections for a positive  $\mu$ . Hence, we can see that the EW and QCD contributions are comparable for diagonal pair production

Stop-sbottom pair production is dominated by the  $W$  exchange diagram with  $u\bar{d}$ -initiated subprocess. The charged-Higgs contribution through  $c\bar{b}$ -initiated subprocess can get to comparable size of cross section at very large  $\tan\beta \gtrsim 35$ , as shown in Fig. 7. Note that the charged-Higgs couples to the  $c\bar{b}$  quarks with an enhancement from  $\tan\beta$  but also with a suppression from  $V_{cb}$ . As we can see, large  $\tan\beta$  limit overcome easily the  $V_{cb}$  suppression.

## V. CONCLUSIONS

We have reviewed the theoretical status of squark pair production at the LHC. The evaluation of the full electroweak contributions has been described in details. The Higgs effect enhance the cross section by about 10-25%, which is comparable to the size of NLO

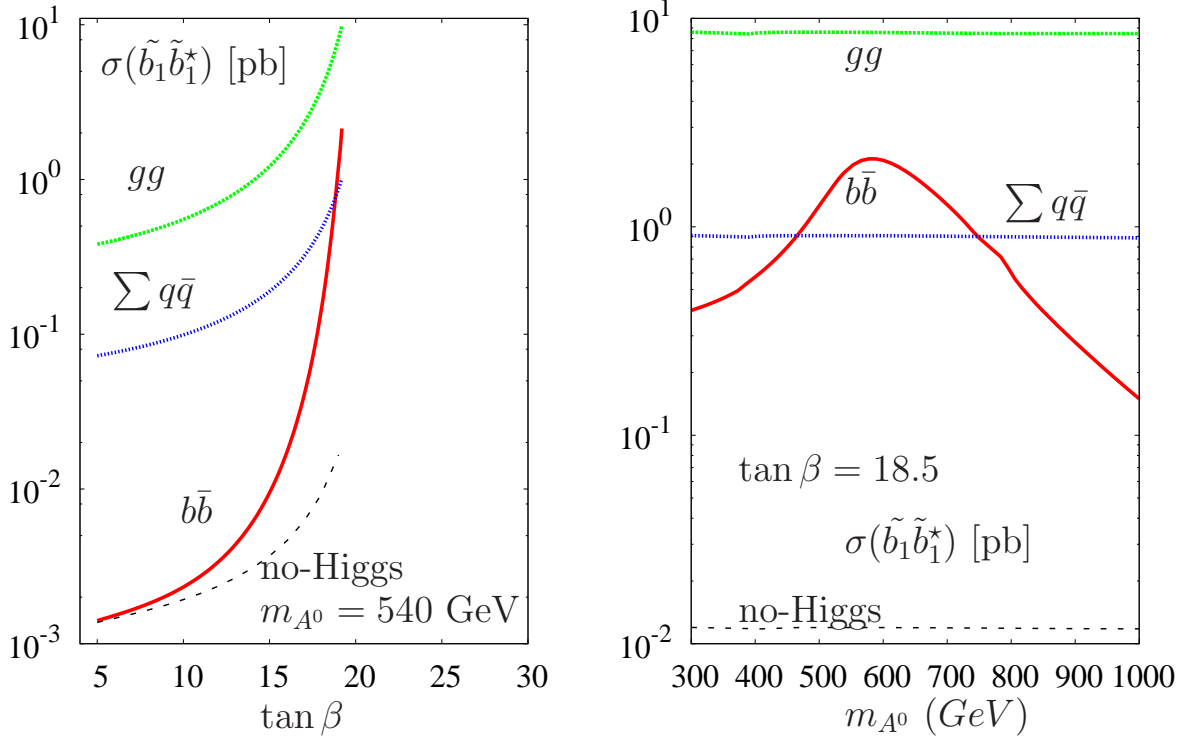


FIG. 3: Production rates for  $\tilde{b}_1\tilde{b}_1^*$  pair production as a function of (left)  $\tan\beta$  and (right)  $m_{A^0}$ . Other SUSY parameters are chosen to be  $M_{SUSY} = 490$  GeV,  $M_2 = 200$  GeV,  $m_{\tilde{g}} = -\mu = 1$  TeV,  $A_0 = 1140$  GeV.

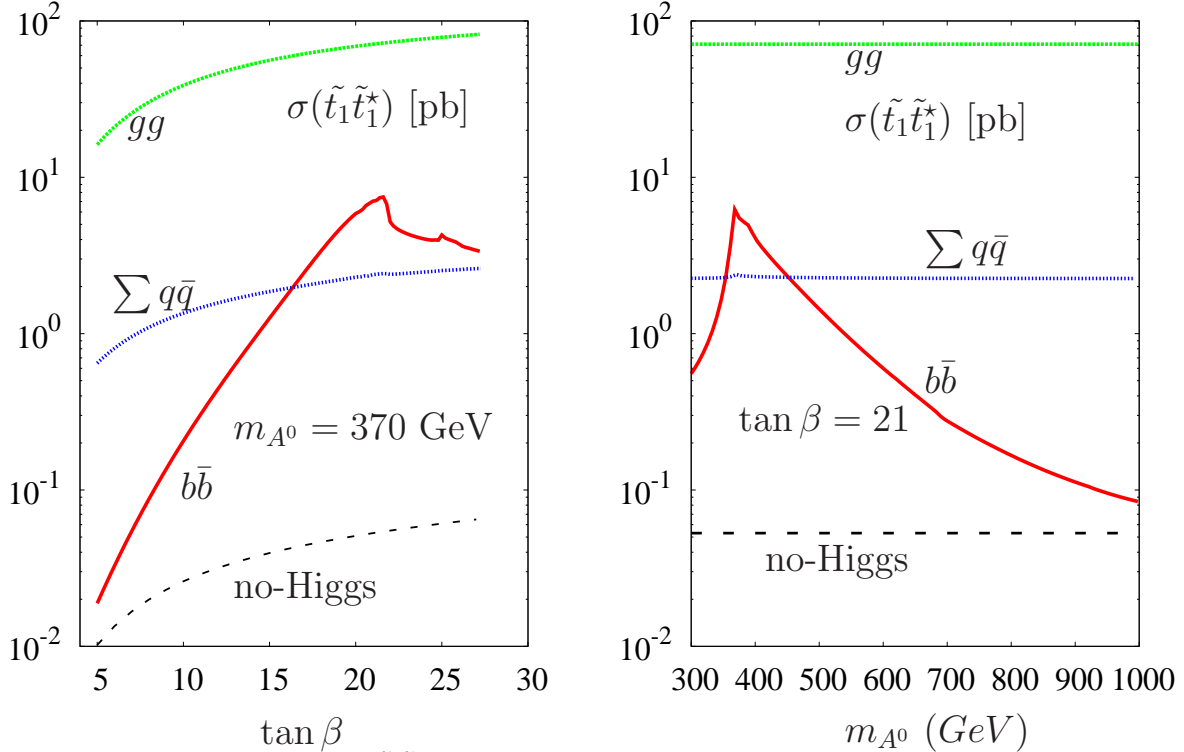


FIG. 4: Production rates for  $\tilde{t}_1\tilde{t}_1^*$  pair production as a function of (left)  $\tan\beta$  and (right)  $m_{A^0}$ . Other SUSY parameters are chosen to be  $M_{SUSY} = 350$  GeV,  $M_2 = 200$  GeV,  $m_{\tilde{g}} = 550$  GeV,  $\mu = -960$  GeV,  $A_0 = 750$  GeV.

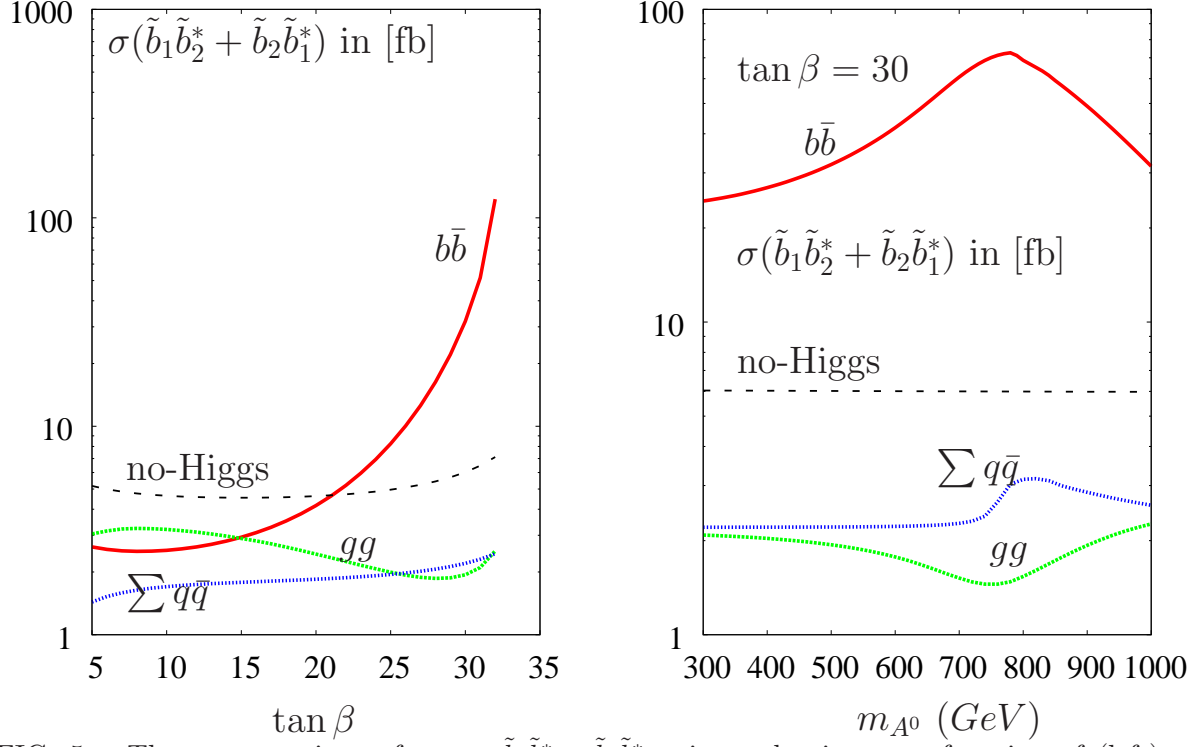


FIG. 5: The cross sections of  $pp \rightarrow \tilde{b}_1\tilde{b}_2^* + \tilde{b}_2\tilde{b}_1^*$  pair production as a function of (left)  $\tan\beta$  and (right)  $m_{A^0}$ . The SUSY parameters are chosen to be  $M_{SUSY} = 400$  GeV,  $M_2 = 200$  GeV,  $m_{\tilde{g}} = 1000$  GeV,  $\mu = -500$  GeV,  $A_0 = 500$  GeV.

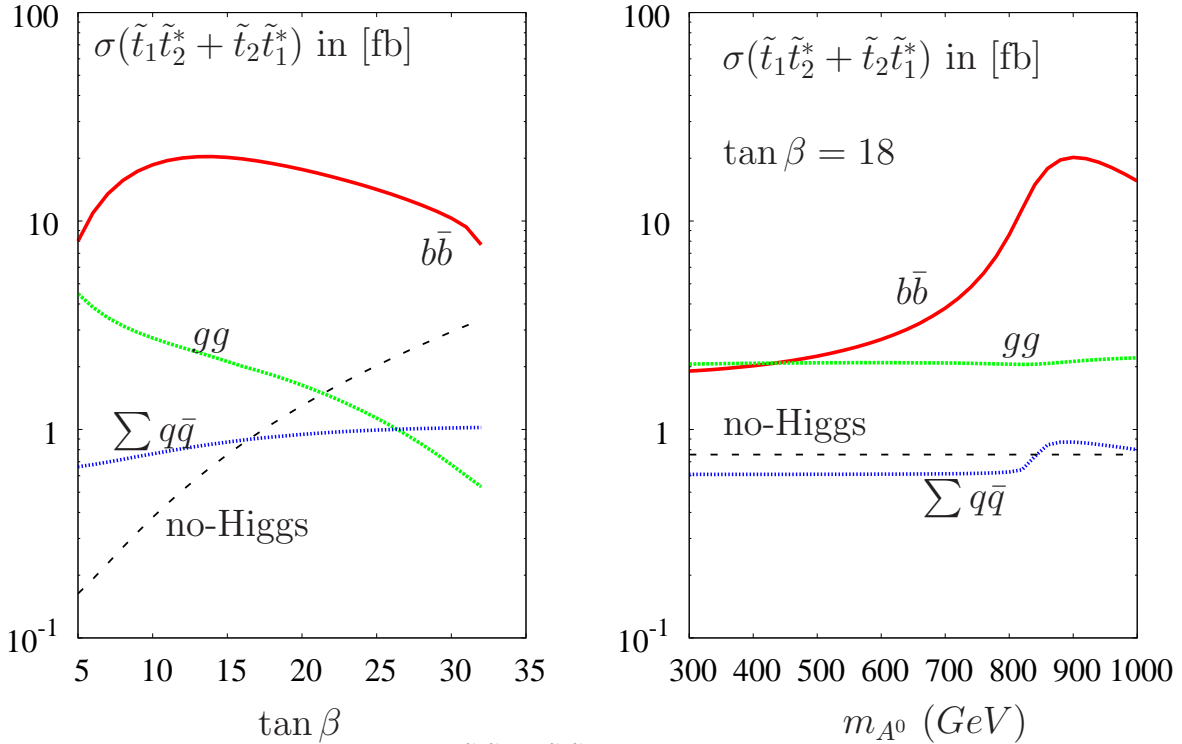


FIG. 6: The cross sections of  $pp \rightarrow \tilde{t}_1\tilde{t}_2^* + \tilde{t}_2\tilde{t}_1^*$  pair production as a function of (left)  $\tan\beta$  and (right)  $m_{A^0}$ . The SUSY parameters are chosen to be  $M_{SUSY} = 400$  GeV,  $M_2 = 200$  GeV,  $m_{\tilde{g}} = 1$  TeV,  $\mu = -500$  GeV,  $A_0 = 500$  GeV.

$\sigma$ [fb]	$\mu < 0, \quad \Delta_b = -0.76$				$\mu > 0, \quad \Delta_b = 0.66$			
	QCD	EW	Higgs	Total	QCD	EW	Higgs	Total
$b\bar{b} \rightarrow \tilde{b}_1 \tilde{b}_1^*$	11.7	16.6	410.2	437.10	0.37	1.24	0.007	1.68
$b\bar{b} \rightarrow \tilde{t}_1 \tilde{t}_1^*$	4.5	3.10	201.8	210.80	2.80	2.21	7.01	9.70
$b\bar{b} \rightarrow \tilde{b}_1 \tilde{b}_2^* + \text{h.c.}$	-	2.65	110.7	125.10	-	1.81	0.52	3.23
$b\bar{b} \rightarrow \tilde{t}_1 \tilde{t}_2^* + \text{h.c.}$	-	0.47	9.8	10.80	-	0.43	8.35	9.60
$c\bar{b} \rightarrow \tilde{t}_1 \tilde{b}_1^*$	-	$0.76 \times 10^{-3}$	27.85	27.86	-	$0.94 \times 10^{-4}$	$1.71 \times 10^{-2}$	$1.72 \times 10^{-2}$
$u\bar{d} \rightarrow \tilde{t}_1 \tilde{b}_1^*$	-	10.16	45.95	56.21	-	1.77	$6 \times 10^{-2}$	1.84
$c\bar{b} \rightarrow \tilde{t}_1 \tilde{b}_2^* + \text{h.c.}$	-	$0.36 \times 10^{-4}$	0.32	0.33	-	$0.83 \times 10^{-4}$	$2.72 \times 10^{-2}$	$2.73 \times 10^{-2}$
$u\bar{d} \rightarrow \tilde{t}_1 \tilde{b}_2^* + \text{h.c.}$	-	$4.8 \times 10^{-2}$	1.71	1.72	-	$0.25 \times 10^{-2}$	0.87	0.88

TABLE I: The effect of the sign of the  $\mu$  parameter on the production cross sections (in fb). The SUSY parameters are chosen to be  $A_0 = m_{\tilde{g}} = |\mu| = 1$  TeV,  $M_{SUSY} = 490$  GeV and  $M_2 = 200$  GeV,  $\tan\beta = 20$  and the Higgs masses are taken at the resonance.

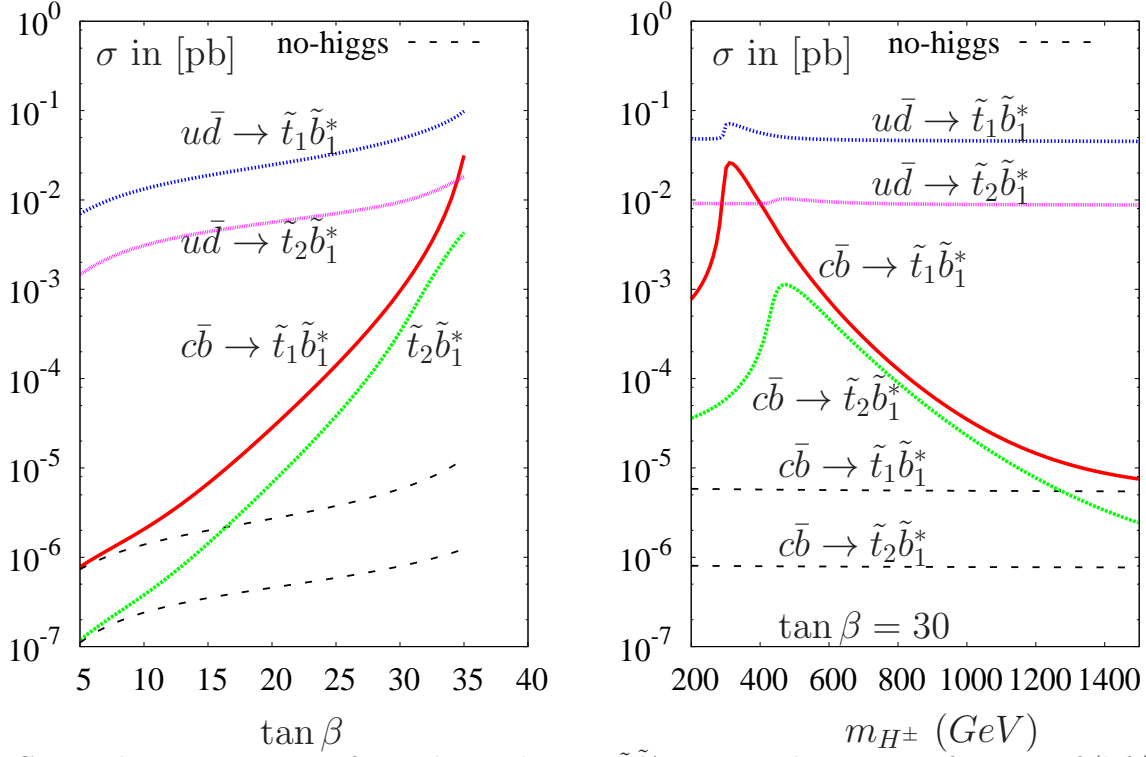


FIG. 7: The cross sections of mixed squark  $pp \rightarrow \tilde{t}_i \tilde{b}_j^*$  pairs production as a function of (left)  $\tan\beta$  and (right)  $m_{H^\pm}$ . The SUSY parameters are chosen to be  $M_{SUSY} = 200$  GeV,  $M_2 = 200$  GeV,  $m_{\tilde{g}} = 1000$  GeV,  $\mu = -200$  GeV,  $A_0 = 200$  GeV. Note that for non-diagonal production  $qq' \rightarrow \tilde{t}_i \tilde{b}_j^*$  we have taken into account their hermetic conjugate.

correction as well as to the PDF uncertainties. In the case of non-diagonal squarks production, we have seen some enhancement for large  $\tan\beta$ . Those processes can be used to extract some information on the squarks mixing angles. One concludes that LO electroweak contribution has to be taken into account for any reliable prediction.

## Acknowledgments

A.A is supported by the National Science of Theoretical Studies-Taipei under contract # 980528731. R.B is supported by National Cheng Kung University Grant No. HUA 97-03-02-063. R.B acknowledges the KEK theory exchange program for physicists in Taiwan and the very kind hospitality at KEK. K.C. was supported in parts by the NSC under Grant Nos. (96-2628-M-007-002-MY3), by the NCTS, by the Boost Program of the NTHU, and by WCU program through the NRF funded by the MEST (R31-2008-000-10057-0). T.C. was supported by the NSC under Grant no. 98-2112-M-001-014-MY3.

## APPENDIX A: FEYNMAN RULES

In this appendix, we give the relevant Feynman rules for our study.

### 1. Higgs-squark couplings

In this appendix we collect the couplings of the  $h^0$ ,  $H^0$  and  $A^0$  bosons to the squarks  $\tilde{q}_i$  with  $q = t, b$  and  $i = 1, 2$ , which are relevant for our analysis. by using the mixing matrix which rotates the left- and right-handed squark fields  $\tilde{q}_L$  and  $\tilde{q}_R$ , into mass eigenstates  $\tilde{q}_i$  as Squark couplings to Higgs boson are given by where  $\alpha$  is the mixing angle in the neutral Higgs sector, we have used  $c_\alpha = \cos \alpha$ ,  $s_\alpha = \sin \alpha$ ,  $c_{\alpha+\beta} = \cos(\alpha + \beta)$ ,  $s_{\alpha+\beta} = \sin(\alpha + \beta)$ ,  $s_\beta = \sin \beta$  and  $c_\beta = \cos \beta$  as abbreviations. We note the following properties of the above couplings  $g_{h^0\tilde{q}_1\tilde{q}_2} = g_{h^0\tilde{q}_2\tilde{q}_1}$ ,  $g_{H^0\tilde{q}_1\tilde{q}_2} = g_{H^0\tilde{q}_2\tilde{q}_1}$  and  $g_{A^0\tilde{q}_1\tilde{q}_2} = -g_{A^0\tilde{q}_2\tilde{q}_1}$ . Squark couplings to quarks and either charginos  $\tilde{\chi}^\pm$  or neutralinos  $\tilde{\chi}^0$  are straightforward, but somewhat more complicated by the mixing angles associated with the  $\tilde{\chi}^\pm$  and  $\tilde{\chi}^0$  mass eigenstates.

#### a. Squark - Squark - $h^0$

$$\hat{G}_1 = \begin{pmatrix} \frac{g m_Z}{c_W} C_{qL} s_{\alpha+\beta} - \sqrt{2} m_q Y^q \begin{Bmatrix} c_\alpha \\ -s_\alpha \end{Bmatrix} & -\frac{1}{\sqrt{2}} Y^q \left( A_q \begin{Bmatrix} c_\alpha \\ -s_\alpha \end{Bmatrix} + \mu \begin{Bmatrix} s_\alpha \\ c_\alpha \end{Bmatrix} \right) \\ -\frac{1}{\sqrt{2}} Y^q \left( A_q \begin{Bmatrix} c_\alpha \\ -s_\alpha \end{Bmatrix} + \mu \begin{Bmatrix} s_\alpha \\ c_\alpha \end{Bmatrix} \right) & \frac{g m_Z}{c_W} C_{qR} s_{\alpha+\beta} - \sqrt{2} m_q Y^q \begin{Bmatrix} c_\alpha \\ -s_\alpha \end{Bmatrix} \end{pmatrix} \quad (\text{A1})$$

for  $\left\{ \begin{smallmatrix} \text{up} \\ \text{down} \end{smallmatrix} \right\}$  type squarks respectively.  $\alpha$  is the mixing angle in the CP even neutral Higgs boson sector.  $Y^q$  are the Yukawa couplings:

$$Y^t = \frac{g m_t}{\sqrt{2} m_W \sin \beta}, \quad Y^b = \frac{g m_b}{\sqrt{2} m_W \cos \beta}. \quad (\text{A2})$$



b. *Squark - Squark - H<sup>0</sup>*

$$\hat{G}_2 = \begin{pmatrix} -\frac{g m_Z}{c_W} C_{qL} c_{\alpha+\beta} - \sqrt{2} m_q Y^q \begin{Bmatrix} s_\alpha \\ c_\alpha \end{Bmatrix} & -\frac{1}{\sqrt{2}} Y^q (A_q \begin{Bmatrix} s_\alpha \\ c_\alpha \end{Bmatrix} - \mu \begin{Bmatrix} c_\alpha \\ s_\alpha \end{Bmatrix}) \\ -\frac{1}{\sqrt{2}} Y^q (A_q \begin{Bmatrix} s_\alpha \\ c_\alpha \end{Bmatrix} - \mu \begin{Bmatrix} c_\alpha \\ s_\alpha \end{Bmatrix}) & -\frac{g m_Z}{c_W} C_{qR} s_{\alpha+\beta} - \sqrt{2} m_q Y^q \begin{Bmatrix} s_\alpha \\ c_\alpha \end{Bmatrix} \end{pmatrix} \quad (\text{A3})$$

Notice that  $G_2$  can be obtained from  $G_1$  by the replacement  $\alpha \rightarrow \alpha + \pi/2$ , i.e.  $c_\alpha \rightarrow s_\alpha$  and  $s_\alpha \rightarrow -c_\alpha$ .

c. *Squark - Squark - A<sup>0</sup>*

$$\hat{G}_3 = i \frac{g m_q}{2 m_W} \begin{pmatrix} 0 & -A_q \begin{Bmatrix} \cot \beta \\ \tan \beta \end{Bmatrix} - \mu \\ A_q \begin{Bmatrix} \cot \beta \\ \tan \beta \end{Bmatrix} + \mu & 0 \end{pmatrix} \quad (\text{A4})$$

d. *Squark - Squark - G<sup>0</sup>*

$$\hat{G}_4 = i \frac{g m_q}{2 m_W} \begin{pmatrix} 0 & -A_q + \mu \begin{Bmatrix} \cot \beta \\ \tan \beta \end{Bmatrix} \\ A_q - \mu \begin{Bmatrix} \cot \beta \\ \tan \beta \end{Bmatrix} & 0 \end{pmatrix} \quad (\text{A5})$$

e. *squark - squark - H<sup>±</sup>*

$$\hat{G}_5^{\tilde{t}} = (\hat{G}_5^{\tilde{b}})^T = \frac{g}{\sqrt{2} m_W} \begin{pmatrix} m_b^2 \tan \beta + m_t^2 \cot \beta - m_W^2 s_{2\beta} & m_t (A_t \cot \beta + \mu) \\ m_b (A_b \tan \beta + \mu) & 2 m_t m_b / \sin 2\beta \end{pmatrix} \quad (\text{A6})$$

f. *squark - squark - G<sup>±</sup>*

$$\hat{G}_6^{\tilde{t}} = (\hat{G}_6^{\tilde{b}})^T = \frac{g}{\sqrt{2} m_W} \begin{pmatrix} m_t^2 - m_b^2 - m_W^2 c_{2\beta} & m_t (A_t - \mu \cot \beta) \\ m_b (\mu \tan \beta - A_b) & 0 \end{pmatrix} \quad (\text{A7})$$

## 2. quark-Squark-neutralino and quark-Squark-chargino

### a. quark – squark – neutralino

$$\mathcal{A}_{im}^{\tilde{q}} = -\frac{1}{3\sqrt{2}c_W s_\beta s_W} \left\{ \begin{array}{l} -4m_W s_\beta R_{i2}^{\tilde{u}} N_{m1}^* + 3c_W m_u N_{m4}^* R_{i1}^{\tilde{u}} \\ 2c_\beta M_W s_W N_{m1}^* R_{i2}^{\tilde{d}} + 3c_W m_d N_{m3}^* R_{i1}^{\tilde{d}} \end{array} \right\}, \quad (\text{A8})$$

$$\mathcal{B}_{im}^{\tilde{q}} = -\frac{1}{3\sqrt{2}c_W s_\beta s_W} \left\{ \begin{array}{l} 3c_W m_u N_{m4} R_{i2}^{\tilde{u}} + m_W s_\beta R_{i1}^{\tilde{u}} (s_W N_{m1} + 3c_W N_{m2}) \\ 3c_W m_d R_{i2}^{\tilde{d}} N_{m3} + c_\beta m_W R_{i1}^{\tilde{d}} (s_W N_{m1} - 3c_W N_{m2}) \end{array} \right\} \quad (\text{A9})$$

Here  $N$  is the  $4 \times 4$  unitary matrix diagonalizing the neutral gaugino-higgsino mass matrix [1].

### b. quark – squark – chargino

$$\mathcal{L}_{ik}^{\tilde{q}} = U_{k2}^* U_{i1}^* \left\{ \begin{array}{l} \frac{m_d}{\sqrt{2}c_\beta m_W} \\ \frac{m_u}{\sqrt{2}s_\beta m_W} \end{array} \right\}, \quad \mathcal{K}_{ik}^{\tilde{q}} = - \left\{ \begin{array}{l} \frac{1}{2m_W s_\beta} (2m_W s_\beta R_{i1}^{\tilde{u}} V_{k1} - \sqrt{2}m_u R_{i2}^{\tilde{u}} V_{k2}) \\ \frac{1}{2m_W c_\beta} (2m_W c_\beta R_{i1}^{\tilde{d}} U_{k1} - \sqrt{2}m_d R_{i2}^{\tilde{d}} U_{k2}) \end{array} \right\}. \quad (\text{A10})$$

Here  $U$  and  $V$  are the  $2 \times 2$  unitary matrices diagonalizing the charged gaugino–higgsino mass matrix [1].

## APPENDIX B: PRODUCTION RATES

The production of squark pairs, as initiated by  $b\bar{b}$  annihilation, involves gluon, photon, Z,  $W$  and Higgs bosons in the s-channel as well as gluino and neutralino exchanges in the t-channel. Since left- and right-squarks generally have different masses we present the differential cross section for each subprocess separately in the mass basis. The spin and color averages are taken into account.  $i, j = 1 \dots 2$ ,  $m, n = 1 \dots 4$  and  $k, l = 1 \dots 2$ .

1.  $b\bar{b} \rightarrow \tilde{b}_i \tilde{b}_j^*$

The differential cross section for  $b\bar{b} \rightarrow \tilde{b}_i \tilde{b}_i^*$  (diagonal) is given by

$$\begin{aligned}
\frac{d\hat{\sigma}(b\bar{b} \rightarrow \tilde{b}_i \tilde{b}_i^*)}{d\hat{t}} &= \frac{2\pi}{9\hat{s}^2} \left( \hat{t}\hat{u} - m_{\tilde{b}_i}^4 \right) \tag{B1} \\
&\times \left[ \frac{2\alpha_s^2}{\hat{s}^2} + \frac{9\alpha^2}{\hat{s}^2} e_b^4 + \left( \frac{4\alpha\alpha_s e_b^2}{\hat{s}(\hat{t} - m_{\tilde{g}}^2)} - \frac{2\alpha_s^2}{3\hat{s}(\hat{t} - m_{\tilde{g}}^2)} \right) [(\mathcal{R}_{i1}^{\tilde{b}})^2 + (\mathcal{R}_{i2}^{\tilde{b}})^2] \right. \\
&+ \frac{[(\mathcal{A}_{ik}^{\tilde{b}})^2 + (\mathcal{B}_{ik}^{\tilde{b}})^2]}{(\hat{t} - m_{\tilde{\chi}_0^0}^2)} \left( \frac{3\alpha^2 e_b^2}{2\hat{s}} + \frac{2\alpha\alpha_s}{\hat{s}} \right) + \frac{3\alpha^2 e_b}{2} \frac{(\hat{s} - M_Z^2)}{\hat{s}} D_Z^2 g_{Z\tilde{q}_i\tilde{q}_i} \\
&- \frac{3\alpha^2 e_b}{2\hat{s}} \frac{(\hat{u} - \hat{t})}{(\hat{t}\hat{u} - m_{\tilde{b}_i}^4)} \left( (\hat{s} - M_h^2) g_{hbb} D_h(G_1)_{ii} + (\hat{s} - M_H^2) g_{Hbb} D_H(G_2)_{ii} \right) \\
&+ \frac{9\alpha^2}{4} (C_{qL}^2 + C_{qR}^2) g_{Z\tilde{b}_i\tilde{b}_i}^2 D_Z^2 + \frac{2\alpha\alpha_s}{3} (C_{qL}(\mathcal{R}_{i1}^{\tilde{b}})^2 + C_{qR}(\mathcal{R}_{i2}^{\tilde{b}})^2) g_{Z\tilde{b}_i\tilde{b}_i} D_Z^2 \frac{(\hat{s} - M_Z^2)}{(\hat{t} - m_{\tilde{g}}^2)} \\
&+ \frac{9\alpha^2}{4(\hat{t}\hat{u} - m_{\tilde{b}_i}^4)} \left| g_{hbb} D_h(G_1)_{ii} + g_{Hbb} D_H(G_2)_{ii} \right|^2 \\
&+ \frac{\alpha_s^2}{(\hat{t} - m_{\tilde{g}}^2)^2} \left[ (\mathcal{R}_{i1}^{\tilde{q}})^4 + (\mathcal{R}_{i2}^{\tilde{q}})^4 + \frac{2m_{\tilde{g}}^2 \hat{s}}{(\hat{t}\hat{u} - m_{\tilde{b}_i}^4)} (\mathcal{R}_{i1}^{\tilde{q}})^2 (\mathcal{R}_{i2}^{\tilde{q}})^2 \right] \\
&+ \frac{9\alpha^2}{8(\hat{t} - m_{\tilde{\chi}_k^0}^2)(\hat{t} - m_{\tilde{\chi}_m^0}^2)} \left[ (\mathcal{A}_{ik}^{\tilde{q}})^4 + (\mathcal{B}_{im}^{\tilde{q}})^4 + \frac{2m_{\tilde{\chi}_k^0} m_{\tilde{\chi}_m^0} \hat{s}}{(\hat{t}\hat{u} - m_{\tilde{b}_i}^4)} (\mathcal{A}_{ik}^{\tilde{q}})^2 (\mathcal{B}_{im}^{\tilde{q}})^2 \right] \\
&+ \left[ \frac{\alpha\alpha_s}{3} \frac{\hat{s}m_{\tilde{g}}}{(\hat{t} - m_{\tilde{g}}^2)} (\mathcal{R}_{i1}^{\tilde{q}})(\mathcal{R}_{i2}^{\tilde{q}}) - \frac{4\alpha^2}{3} g_{Z\tilde{q}_i\tilde{q}_i} (C_{qL} + C_{qR})(\hat{s} - M_Z^2)(\hat{u} - \hat{t}) D_Z \right] \\
&\times \frac{1}{(\hat{t}\hat{u} - m_{\tilde{b}_i}^4)} \left[ (\hat{s} - m_h^2) g_{hbb} D_h(G_1)_{ii} + (\hat{s} - m_H^2) g_{Hbb} D_H(G_2)_{ii} \right] \\
&- \frac{\alpha^2 g_{Z\tilde{q}_i\tilde{q}_i}}{4} \frac{[(\mathcal{A}_{ik}^{\tilde{q}})^2 C_{bL} + (\mathcal{B}_{ik}^{\tilde{q}})^2 C_{bR}]}{(\hat{t} - m_{\tilde{\chi}_k^0}^2)} (\hat{s} - M_Z^2) D_Z^2 \\
&+ \frac{3\alpha^2}{4(\hat{t} - m_{\tilde{\chi}_k^0}^2)} \mathcal{A}_{ik}^{\tilde{q}} \mathcal{B}_{ik}^{\tilde{q}} m_{\tilde{\chi}_k^0} \hat{s} \left[ (\hat{s} - M_{h^0}^2) g_{hbb} D_h^2(G_1)_{ii} + (\hat{s} - M_{H^0}^2) g_{Hbb} D_H^2(G_2)_{ii} \right]
\end{aligned}$$

Where  $D_\Phi^{-1} = \hat{s} - m_\Phi^2 + im_\Phi \Gamma_\Phi$ . The imaginary part in the  $D_\Phi^{-1}$  is the Breit-Wigner prescription for regulating the  $\Phi$  pole.

while the differential cross section for off-diagonal ( $i \neq j$ ) is given by

$$\begin{aligned}
\frac{d\hat{\sigma}(b\bar{b} \rightarrow \tilde{b}_i \tilde{b}_j^*)}{d\hat{t}} &= \frac{2\pi}{9\hat{s}^2} \left( \hat{t}\hat{u} - m_{\tilde{q}_i}^2 m_{\tilde{q}_j}^2 \right) \left[ \frac{9\alpha^2}{4} (C_{qL}^2 + C_{qR}^2) g_{Z\tilde{q}_i\tilde{q}_j}^2 D_Z^2 \right. \\
&+ \frac{2\alpha\alpha_s}{3} (C_{qL}(\mathcal{R}_{i1}^{\tilde{q}})^2 + C_{qR}(\mathcal{R}_{j2}^{\tilde{q}})^2) g_{Z\tilde{q}_i\tilde{q}_j} D_Z^2 \frac{(\hat{s} - M_Z^2)}{(\hat{t} - m_{\tilde{g}}^2)} \\
&+ \frac{1}{\left( \hat{t}\hat{u} - m_{\tilde{q}_i}^2 m_{\tilde{q}_j}^2 \right)} \frac{9\alpha^2}{16} \left| g_{hbb} D_h(G_1)_{ij} + g_{Hbb} D_H(G_2)_{ij} \right|^2 \\
&+ \frac{\alpha_s^2}{(\hat{t} - m_{\tilde{g}}^2)^2} \left[ (\mathcal{R}_{i1}^{\tilde{q}})^4 + (\mathcal{R}_{j2}^{\tilde{q}})^4 + \frac{2m_{\tilde{g}}^2 \hat{s}}{\left( \hat{t}\hat{u} - m_{\tilde{q}_i}^2 m_{\tilde{q}_j}^2 \right)} (\mathcal{R}_{i1}^{\tilde{q}})^2 (\mathcal{R}_{j2}^{\tilde{q}})^2 \right] \\
&+ \frac{9\alpha^2}{8(\hat{t} - m_{\tilde{\chi}_k^0}^2)(\hat{t} - m_{\tilde{\chi}_m^0}^2)} \left[ (\mathcal{A}_{ik}^{\tilde{q}})^4 + (\mathcal{B}_{jm}^{\tilde{q}})^4 + \frac{2m_{\tilde{\chi}_k^0} m_{\tilde{\chi}_m^0} \hat{s}}{\left( \hat{t}\hat{u} - m_{\tilde{q}_i}^2 m_{\tilde{q}_j}^2 \right)} (\mathcal{A}_{ik}^{\tilde{q}})^2 (\mathcal{B}_{jm}^{\tilde{q}})^2 \right] \\
&+ \left[ \frac{\alpha\alpha_s}{3} \frac{\hat{s}m_{\tilde{g}}}{(\hat{t} - m_{\tilde{g}}^2)} (\mathcal{R}_{i1}^{\tilde{q}})(\mathcal{R}_{j2}^{\tilde{q}}) - \frac{4\alpha^2}{3} g_{Z\tilde{q}_i\tilde{q}_j} (C_{qL} + C_{qR})(\hat{s} - M_Z^2)(\hat{u} - \hat{t}) D_Z \right] \\
&\times \frac{1}{\left( \hat{t}\hat{u} - m_{\tilde{q}_i}^2 m_{\tilde{q}_j}^2 \right)} \left[ (\hat{s} - m_h^2) g_{hbb} D_h(G_1)_{ij} + (\hat{s} - m_H^2) g_{Hbb} D_H(G_2)_{ij} \right] \\
&- \frac{\alpha^2 g_{Z\tilde{q}_i\tilde{q}_j}}{4} \frac{[(\mathcal{A}_{ik}^{\tilde{q}})^2 C_{bL} + (\mathcal{B}_{jk}^{\tilde{q}})^2 C_{bR}]}{(\hat{t} - m_{\tilde{\chi}_k^0}^2)} (\hat{s} - M_Z^2) D_Z^2 \\
&+ \frac{3\alpha^2}{4(\hat{t} - m_{\tilde{\chi}_k^0}^2)} \mathcal{A}_{ik}^{\tilde{q}} \mathcal{B}_{jk}^{\tilde{q}} m_{\tilde{\chi}_k^0} \hat{s} \left[ (\hat{s} - M_{h^0}^2) g_{hbb} D_h^2(G_1)_{ij} + (\hat{s} - M_{H^0}^2) g_{Hbb} D_H^2(G_2)_{ij} \right]
\end{aligned} \tag{B2}$$

where summations over  $i, j$ .

a.  $b\bar{b} \rightarrow \tilde{t}_i \tilde{t}_j^*$

Similarly, the differential cross sections for  $\tilde{t}_i \tilde{t}_i^*$  and  $\tilde{t}_i \tilde{t}_j^*$  are respectively given by

$$\begin{aligned}
\frac{d\hat{\sigma}(b\bar{b} \rightarrow \tilde{t}_i \tilde{t}_i^*)}{d\hat{t}} &= \frac{2\pi}{9\hat{s}^2} \left( \hat{t}\hat{u} - m_{\tilde{t}_i}^4 \right) \left[ \frac{2\alpha_s^2}{s^2} + \frac{e_t^2 \alpha^2}{\hat{s}^2} + \frac{\alpha^2}{8} (C_{bL}^2 + C_{bR}^2) g_{Z\tilde{t}_i \tilde{t}_i}^2 D_Z^2 \right. \\
&+ \frac{9\hat{s}\alpha^2}{4(\hat{t}\hat{u} - m_{\tilde{t}_i}^4)} \left| g_{h\tilde{t}_i \tilde{t}_i} g_{hbb} D_h + g_{H\tilde{t}_i \tilde{t}_i} g_{Hbb} D_H \right|^2 \\
&+ \frac{9\alpha^2}{8(\hat{t} - m_{\tilde{\chi}_k^+}^2)(\hat{t} - m_{\tilde{\chi}_l^+}^2)} \left( (\mathcal{L}_{ik}^{\tilde{t}})^4 + (\mathcal{K}_{il}^{\tilde{t}})^4 + \frac{2m_{\tilde{\chi}_k^+} m_{\tilde{\chi}_l^+} \hat{s}}{(\hat{t}\hat{u} - m_{\tilde{t}_i}^4)} (\mathcal{L}_{ik}^{\tilde{t}})^2 (\mathcal{K}_{il}^{\tilde{t}})^2 \right) \\
&+ \frac{2\alpha\alpha_s}{\hat{s}} \frac{[(\mathcal{L}_{ik}^{\tilde{t}})^2 + (\mathcal{K}_{il}^{\tilde{t}})^2]}{(\hat{t} - m_{\tilde{\chi}_k^+}^2)} + \frac{\alpha^2 e_t}{6\hat{s}} (C_{bL} + C_{bR}) g_{Z\tilde{t}_i \tilde{t}_i} (\hat{s} - M_Z^2) D_Z^2 \\
&- 3\alpha^2 \left[ \frac{\hat{s}}{2} \frac{(\mathcal{L}_{ik}^{\tilde{t}} \mathcal{K}_{ik}^{\tilde{t}}) m_{\tilde{\chi}_k^+}}{(\hat{t} - m_{\tilde{\chi}_k^+}^2)} - \frac{(\hat{t} - \hat{u})}{(\hat{t}\hat{u} - m_{\tilde{t}_i}^4)} \left( \frac{e_t}{\hat{s}} - \frac{3}{2} g_{Z\tilde{t}_i \tilde{t}_i} (C_{bL} + C_{bR}) (\hat{s} - M_Z^2) D_Z^2 \right) \right] \\
&\times \left( g_{h\tilde{t}_i \tilde{t}_i} g_{hbb} (\hat{s} - M_h^2) D_h^2 + g_{H\tilde{t}_i \tilde{t}_i} g_{Hbb} (\hat{s} - M_H^2) D_H^2 \right) \\
&- \frac{3\alpha^2}{2} \frac{(\hat{s} - M_Z^2)}{(\hat{t} - m_{\tilde{\chi}_k^+}^2)} \left[ (C_{bL} (\mathcal{K}_{ik}^{\tilde{t}})^2 + C_{bR} (\mathcal{L}_{ik}^{\tilde{t}})^2) D_Z^2 - \frac{\alpha^2}{2\hat{s}} \frac{[(\mathcal{K}_{ik}^{\tilde{t}})^2 + (\mathcal{L}_{ik}^{\tilde{t}})^2]}{(\hat{t} - m_{\tilde{\chi}_k^+}^2)} \right]
\end{aligned} \tag{B3}$$

$$\begin{aligned}
\frac{d\hat{\sigma}(b\bar{b} \rightarrow \tilde{t}_i \tilde{t}_j^*)}{d\hat{t}} &= \frac{2\pi}{9\hat{s}^2} \left( \hat{t}\hat{u} - m_{\tilde{t}_i}^2 m_{\tilde{t}_j}^2 \right) \left[ \frac{\alpha^2}{8} (C_{bL}^2 + C_{bR}^2) g_{Z\tilde{t}_i \tilde{t}_j}^2 D_Z^2 \right. \\
&+ \frac{9\hat{s}\alpha^2}{4(\hat{t}\hat{u} - m_{\tilde{t}_i}^2 m_{\tilde{t}_j}^2)} \left| g_{h\tilde{t}_i \tilde{t}_j} g_{hbb} D_h + g_{H\tilde{t}_i \tilde{t}_j} g_{Hbb} D_H + g_{A\tilde{t}_i \tilde{t}_j} g_{Abb} D_A \right|^2 \\
&+ \frac{9\alpha^2}{8(\hat{t} - m_{\tilde{\chi}_k^+}^2)(\hat{t} - m_{\tilde{\chi}_l^+}^2)} \left( (\mathcal{L}_{ik}^{\tilde{t}})^4 + (\mathcal{K}_{jl}^{\tilde{t}})^4 + \frac{2m_{\tilde{\chi}_k^+} m_{\tilde{\chi}_l^+} \hat{s}}{(\hat{t}\hat{u} - m_{\tilde{t}_i}^2 m_{\tilde{t}_j}^2)} (\mathcal{L}_{ik}^{\tilde{t}})^2 (\mathcal{K}_{jl}^{\tilde{t}})^2 \right) \\
&- 3\alpha^2 \left[ \frac{\hat{s}}{2} \frac{(\mathcal{L}_{ik}^{\tilde{t}} \mathcal{K}_{jk}^{\tilde{t}}) m_{\tilde{\chi}_k^+}}{(\hat{t} - m_{\tilde{\chi}_k^+}^2)} + \frac{3}{2} \frac{(\hat{t} - \hat{u})}{(\hat{t}\hat{u} - m_{\tilde{t}_i}^2 m_{\tilde{t}_j}^2)} \left( g_{Z\tilde{t}_i \tilde{t}_j} (C_{bL} + C_{bR}) (\hat{s} - M_Z^2) D_Z^2 \right) \right] \\
&\times \left( g_{h\tilde{t}_i \tilde{t}_j} g_{hbb} (\hat{s} - M_h^2) D_h^2 + g_{H\tilde{t}_i \tilde{t}_j} g_{Hbb} (\hat{s} - M_H^2) D_H^2 + g_{A\tilde{t}_i \tilde{t}_j} g_{Abb} (\hat{s} - M_A^2) D_A^2 \right) \\
&- \frac{3\alpha^2}{2} \frac{(\hat{s} - M_Z^2)}{(\hat{t} - m_{\tilde{\chi}_k^+}^2)} \left[ (C_{bL} (\mathcal{K}_{jk}^{\tilde{t}})^2 + C_{bR} (\mathcal{L}_{ik}^{\tilde{t}})^2) D_Z^2 \right]
\end{aligned} \tag{B4}$$

## 2. stop-sbottom production

$$\begin{aligned} \frac{d\hat{\sigma}(q\bar{q}' \rightarrow \tilde{t}_i\tilde{b}_j^*)}{d\hat{t}} &= \frac{2\pi}{9\hat{s}^2} |V_{qq'}|^2 |V_{\tilde{t}_i\tilde{b}_j}|^2 \left[ \frac{18\alpha^2}{s_W^4} (\hat{t}u - m_{\tilde{t}_i}^2 m_{\tilde{b}_j}^2) D_W^2 (\mathcal{R}_{i1}^{\tilde{b}} \mathcal{R}_{j1}^{\tilde{t}})^2 \right. \\ &\quad \left. + \frac{9\alpha^2 m_b^2}{8s_W^2} (G_5)_{ij}^2 \hat{s} D_{H^\pm}^2 - \frac{9\alpha^2 m_b^2}{4s_w^2} (\hat{t} - \hat{u}) (G_5)_{ij} D_{H^\pm} D_{W^\pm} \mathcal{R}_{i1}^{\tilde{b}} \mathcal{R}_{j1}^{\tilde{t}} \right] \quad (\text{B5}) \end{aligned}$$

## 3. $gg \rightarrow \tilde{q}_i\tilde{q}_i$

$$\begin{aligned} \frac{d\hat{\sigma}}{d\hat{t}}(gg \rightarrow \tilde{q}_i\tilde{q}_i^*) &= \frac{\pi\alpha_s^2}{12\hat{s}^2} \left[ \frac{2(m_{\tilde{q}}^4 - \hat{t}\hat{u})}{(m_{\tilde{q}}^2 - \hat{t})(m_{\tilde{q}}^2 - \hat{u})} + \frac{9[4\hat{s}(4m_{\tilde{q}}^2 - \hat{s}) + (\hat{u} - \hat{t})^2]}{8\hat{s}^2} + \frac{7}{4} \right. \\ &\quad - \frac{(4m_{\tilde{q}}^2 - \hat{s})^2}{16(m_{\tilde{q}}^2 - \hat{t})(m_{\tilde{q}}^2 - \hat{u})} - \frac{7(4m_{\tilde{q}}^2 + 4\hat{t} - \hat{s})}{32(\hat{t} - m_{\tilde{q}}^2)} - \frac{7(4m_{\tilde{q}}^2 + 4\hat{u} - \hat{s})}{32(\hat{u} - m_{\tilde{q}}^2)} \\ &\quad + \frac{9[(\hat{t} - \hat{u})(4m_{\tilde{q}}^2 + 4\hat{t} - \hat{s}) - 2(m_{\tilde{q}}^2 - \hat{u})(6m_{\tilde{q}}^2 + 2\hat{t} - \hat{s})]}{32\hat{s}(m_{\tilde{q}}^2 - \hat{t})} \\ &\quad \left. - \frac{9[(\hat{t} - \hat{u})(4m_{\tilde{q}}^2 + 4\hat{u} - \hat{s}) + 2(m_{\tilde{q}}^2 - \hat{t})(6m_{\tilde{q}}^2 + 2\hat{u} - \hat{s})]}{32\hat{s}(m_{\tilde{q}}^2 - \hat{u})} \right] \quad (\text{B6}) \end{aligned}$$

- 
- [1] H. E. Haber and G. L. Kane, Phys. Rept. **117** (1985) 75.
  - [2] J. F. Gunion and H. E. Haber, Nucl. Phys. B272, 1 (1986); B278, 449 (1986); B307, 445 (1988); Erratum B402, 567-569 (1993).
  - [3] P. Nath, R. Arnowitt and A. Chamseddine, “Applied N=1 Supergravity”, ITCP Series in Theoretical Physics, World Scientific, Singapore 1984; H.P. Nilles, Phys. Rep. 110 (1984) 1.
  - [4] R. Barate *et al.* [LEP Working Group for Higgs boson searches], Phys. Lett. B **565**, 61 (2003).
  - [5]
  - [6] W. Beenakker, R. Höpker, M. Spira and P. M. Zerwas, Nucl. Phys. B **492**, 51 (1997) [arXiv:hep-ph/9610490]; W. Beenakker, R. Höpker, M. Spira and P. M. Zerwas, Phys. Rev. Lett. **74**, 2905 (1995) [arXiv:hep-ph/9412272]. W. Beenakker, R. Hopker and M. Spira, arXiv:hep-ph/9611232.
  - [7] G. L. Kane and J. P. Leveille, Phys. Lett. B **112**, 227 (1982). P. R. Harrison and C. H. Llewellyn Smith, Nucl. Phys. B **213**, 223 (1983) [Erratum-ibid. B **223**, 542 (1983)]. E. Reya and D. P. Roy, Phys. Rev. D **32**, 645 (1985). S. Dawson, E. Eichten and C. Quigg, Phys. Rev. D **31**, 1581 (1985). H. Baer and X. Tata, Phys. Lett. B **160**, 159 (1985).
  - [8] W. Beenakker, M. Kramer, T. Plehn, M. Spira and P. M. Zerwas, Nucl. Phys. B **515**, 3 (1998) [arXiv:hep-ph/9710451].
  - [9] E. L. Berger, B. W. Harris, D. E. Kaplan, Z. Sullivan, T. M. P. Tait and C. E. M. Wagner, Phys. Rev. Lett. **86**, 4231 (2001) [arXiv:hep-ph/0012001].

- [10] W. Hollik and E. Mirabella, JHEP **0812**, 087 (2008) [arXiv:0806.1433 [hep-ph]]. W. Hollik, E. Mirabella and M. K. Trenkel, JHEP **0902**, 002 (2009) [arXiv:0810.1044 [hep-ph]]. J. Germer, W. Hollik, E. Mirabella and M. K. Trenkel, arXiv:0909.3046 [hep-ph].
- [11] S. Bornhauser, M. Drees, H. K. Dreiner and J. S. Kim, Phys. Rev. D **76**, 095020 (2007) [arXiv:0709.2544 [hep-ph]].
- [12] G. Bozzi, B. Fuks and M. Klasen, Phys. Rev. D **72**, 035016 (2005) [arXiv:hep-ph/0507073]; D. Berdine and D. Rainwater, Phys. Rev. D **72**, 075003 (2005) [arXiv:hep-ph/0506261].
- [13] A. Djouadi, Phys. Rept.**459**:1-241,2008 [arXiv:hep-ph/0503173].
- [14] A. Dedes, S. Heinemeyer, S. Su and G. Weiglein, Nucl. Phys. B **674**, 271 (2003) [arXiv:hep-ph/0302174].
- [15] A. Djouadi, P. Gambino, S. Heinemeyer, W. Hollik, C. Junger and G. Weiglein, Phys. Rev. Lett. **78**, 3626 (1997). [arXiv:hep-ph/9612363].
- [16] M. Drees and K. Hagiwara, Phys. Rev. D **42**, 1709 (1990).
- [17] C. Amsler *et al.* [Particle Data Group], Phys. Lett. B **667**, 1 (2008).
- [18] J. A. Casas, A. Lleyda and C. Munoz, Nucl. Phys. B **471**, 3 (1996) [arXiv:hep-ph/9507294]. J.M. Frère, D.R.T Jones and S. Raby, Nucl.Phys. **B222** (1983) 11. M. Claudson, L. Hall and I. Hinchcliffe, Nucl. Phys. **B228** (1983) 501. C. Kounnas, A.B. Lahanas, D.V. Nanopoulos and M. Quirós, Nucl. Phys. **B236** (1984) 438. J.F. Gunion, H.E. Haber and M. Sher, Nucl. Phys. **B306** (1988) 1. P. Langacker and N. Polonsky, Phys. Rev. **D50** (1994) 5824. A. Strumia, Nucl. Phys. **B482** (1996) 24.
- [19] L. J. Hall, R. Rattazzi and U. Sarid, Phys. Rev. D **50**, 7048 (1994) [arXiv:hep-ph/9306309].
- [20] M. Carena, D. Garcia, U. Nierste and C. E. M. Wagner, Nucl. Phys. B **577**, 88 (2000) [arXiv:hep-ph/9912516].
- [21] M. S. Carena, M. Olechowski, S. Pokorski and C. E. M. Wagner, Nucl. Phys. B **426**, 269 (1994) [arXiv:hep-ph/9402253].
- [22] D. M. Pierce, J. A. Bagger, K. T. Matchev and R. j. Zhang, Nucl. Phys. B **491**, 3 (1997) [arXiv:hep-ph/9606211].
- [23] J. Guasch, P. Hafliger and M. Spira, Phys. Rev. D **68**, 115001 (2003) [arXiv:hep-ph/0305101].
- [24] M. S. Carena, A. Menon, R. Noriega-Papaqui, A. Szyrkman and C. E. M. Wagner, Phys. Rev. D **74**, 015009 (2006) [arXiv:hep-ph/0603106].
- [25] S. G. Gorishnii, A. L. Kataev, S. A. Larin and L. R. Surguladze, Mod. Phys. Lett. A **5**, 2703 (1990). Phys. Rev. D **43**, 1633 (1991). A. Djouadi, M. Spira and P. M. Zerwas, Z. Phys. C **70**, 427 (1996) [arXiv:hep-ph/9511344]. M. Spira, Fortsch. Phys. **46**, 203 (1998) [arXiv:hep-ph/9705337].
- [26] S. Heinemeyer, W. Hollik and G. Weiglein, Comput. Phys. Commun. **124**, 76 (2000) [arXiv:hep-ph/9812320].
- [27] J. S. Lee, M. Carena, J. Ellis, A. Pilaftsis and C. E. M. Wagner, Comput. Phys. Commun. **180**, 312 (2009) [arXiv:0712.2360 [hep-ph]]. J. S. Lee, A. Pilaftsis, M. S. Carena, S. Y. Choi, M. Drees, J. R. Ellis and C. E. M. Wagner, Comput. Phys. Commun. **156**, 283 (2004) [arXiv:hep-ph/0307377].
- [28] P. M. Nadolsky *et al.*, Phys. Rev. D **78**, 013004 (2008) [arXiv:0802.0007 [hep-ph]].
- [29] R. Brock *et al.* [CTEQ Collaboration], Rev. Mod. Phys. **67**, 157 (1995); P. M. Nadolsky *et al.*, Phys. Rev. D **78**, 013004 (2008); J. Pumplin *et al.* JHEP **0207**, 012 (2002).